

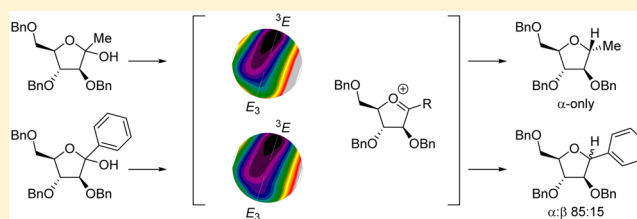
Stereoselectivity in the Lewis Acid Mediated Reduction of Ketofuranoses

Erwin R. van Rijssel,[§] Pieter van Delft,[§] Daan V. van Marle, Stefan M. Bijvoets, Gerrit Lodder, Herman S. Overkleeft, Gijsbert A. van der Marel, Dmitri V. Filippov,* and Jeroen D. C. Codée*

Leiden Institute of Chemistry, Leiden University, P.O. Box 9502, 2300 RA Leiden, The Netherlands

S Supporting Information

ABSTRACT: The Lewis acid mediated reduction of ribose-, arabinose-, xylose-, and lyxose-derived methyl and phenyl ketofuranoses with triethylsilane as nucleophile was found to proceed with good to excellent stereoselectivity to provide the 1,2-*cis* addition products. The methyl ketoses reacted in a more stereoselective manner than their phenyl counterparts. The stereochemical outcome of the reactions parallels the relative stability of the oxocarbenium ion conformers involved, as assessed by calculating the free energy surface maps of their complete conformational space. The Lewis acid mediated reduction allows for a direct synthesis of C-glycosides with predictable stereochemistry.



INTRODUCTION

C-Glycosides are carbohydrate-derived molecules in which the anomeric exocyclic oxygen is substituted for a carbon functionality. C-Glycosides are often used as metabolically stable mimics of naturally occurring O- and N-glycosides, and they can have appealing biological properties, ranging from antibiotic and antiviral activity to anticancer activity.¹ Examples of naturally occurring C-glycosides are the C-nucleoside pseudouridine^{1a–d} and the C-aryl glycoside dapagliflozin.^{1g} The latter compound is the C-glycoside analogue of the naturally occurring O-glycoside phlorizin, and it is currently used in the clinic for the treatment of type 2 diabetes.^{1g} Because of their attractive biological properties, various approaches have been developed for their synthesis. A commonly used strategy to synthesize C-glycosides entails the reaction of glycosyl lactones with an alkyl or aryl nucleophile to give glycosyl hemiketals that are subsequently reduced under Lewis acidic conditions to provide the target compounds.^{1a,b,2} In this process, a new stereogenic center is created and control over the stereochemical course of the reaction is required to enable a productive and effective overall transformation. A notable example is the reduction of perbenzylated ribofuranose ketoses that provides β -linked products in a highly stereoselective fashion.^{2h,3} Scheme 1 depicts a synthesis of pseudouridine that builds on the stereoselective reduction of perbenzylated riboketosides. Reaction of ribonolactone **1** with lithiated pyrimidine **2** gave hemiketal **3** that was reduced with triethylsilane (TES) using $\text{BF}_3 \cdot \text{OEt}_2$ as the Lewis acid. After removal of the *tert*-butyl protecting groups with trifluoroacetic acid (TFA), the desired 1,2-*trans* compound **4** was obtained as a single anomer. The stereoselectivity in the reduction is striking because the nucleophile comes in *cis* with respect to the substituents at C2 and C3.

Presumably, the stereoselectivity is the result of the structure and particular reactivity of the intermediate in the process: the furanosyl oxocarbenium ion. Woerpel and co-workers have devised a two-conformer model in which the equilibrium between the 3E and E_3 furanosyl oxocarbenium ion envelope conformers is decisive in determining the stereoselectivity of reactions involving these intermediates (Figure 1).⁴ Nucleophilic attack on either of the envelopes occurs on the inside to avoid eclipsing interactions with the substituent at C2 and to provide a product featuring a staggered C1–C2 conformation. Reaction on the 3E conformer therefore occurs on the top face, where the E_3 envelope is approached from the bottom face. The equilibrium between the two envelopes is determined by the nature and orientation of the substituents on the tetrahydrofuran ring. Alkoxy substituents at C2 preferentially take up a pseudoequatorial position to allow hyperconjugative stabilization of the oxocarbenium ion by the pseudoaxial C2–H2 bond, while C3-alkoxy substituents are preferentially positioned in a pseudoaxial fashion to allow the donation of electron density into the electron-depleted anomeric center.^{4d,5} In our previous work, we established the relative stability of fully decorated aldofuranosyl oxocarbenium ions.⁶ A complete survey of the energy landscape of the entire conformational space for the four possible pentaaldoses (ribose, arabinose, xylose, and lyxose) provided a clear picture how the three-ring substituents on the furanosyl oxocarbenium ion affect oxocarbenium ion stability and, therefore, their reactivity in addition reactions. Lewis acid mediated substitution reactions of the four possible perbenzylated aldofuranosyl acetates using triethylsilane-*d* as a nucleophile all proceeded in a 1,2-*cis*-selective manner. These results parallel the theoretically

Received: February 23, 2015

Published: March 31, 2015

Scheme 1. Diastereoselective Synthesis of Protected Pseudouridine 4

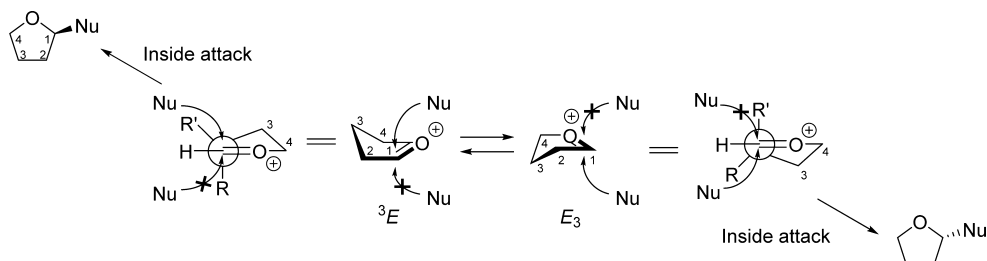
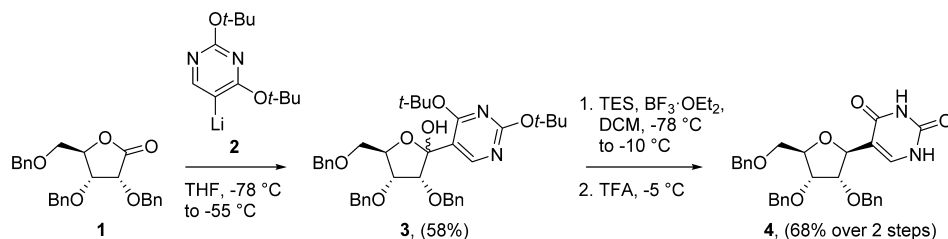
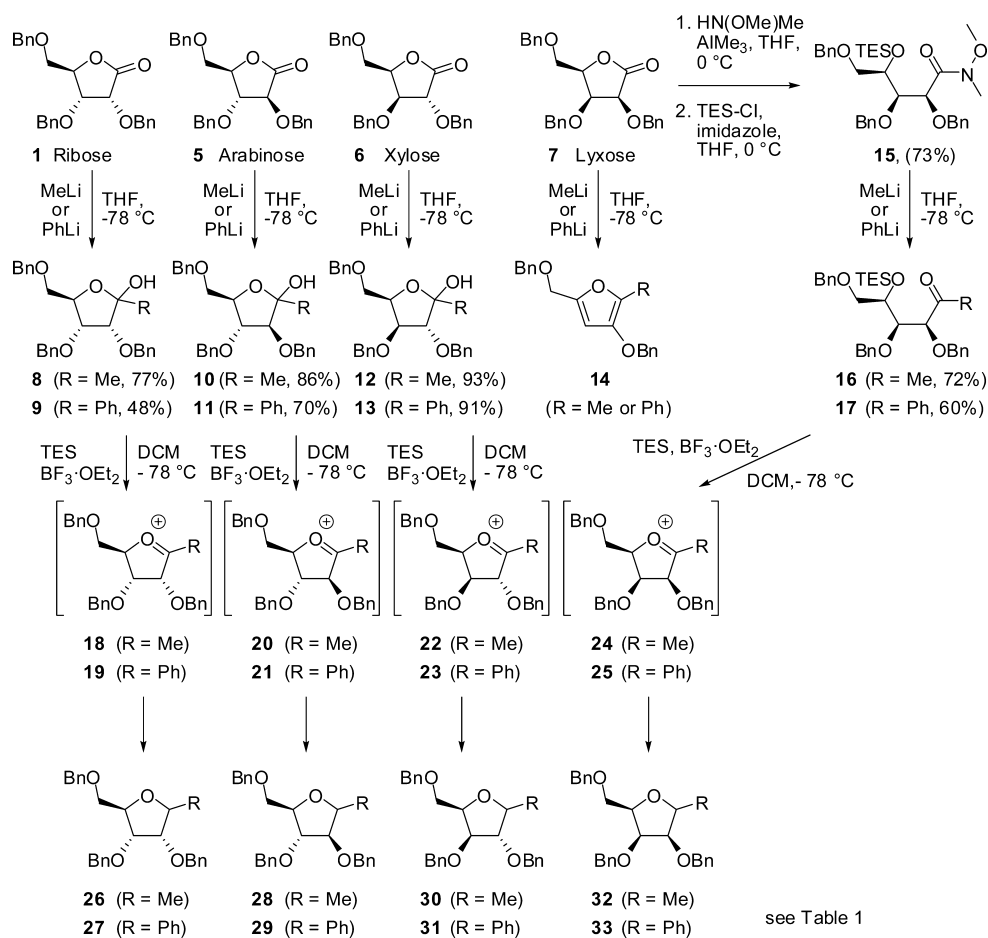


Figure 1. Two-conformer model. Inside attack on either of the two oxocarbenium ions leads to the two epimeric products.

Scheme 2. Synthesis of the Perbenzylated Ribose, Arabinose, and Xylofuranosyl Hemiketals, Lyxose-Configured Ketones, and Their Ensuing Reduction Reactions



predicted relative stability of the intermediate furanosyl oxocarbenium ion conformers.

Given the enhanced stability of tertiary cations over their secondary counterparts, it is likely that ketofuranosyl oxocarbenium ions are involved in the reduction of the C-furanoses described above. To establish how a substituent at

the anomeric center of ketofuranoses influences the stability of the corresponding oxocarbenium ions and their nucleophilic addition reactions, we have investigated the reduction of the methyl and phenyl C-furanoses of four possible pentose configurations, and we have mapped the conformational energy landscape of the intermediate ketofuranosyl oxocarbenium ions.

Table 1. Results of the Lewis Acid Mediated Reductions

Entry	Furanosyl donor	Product		1,2- <i>trans</i> : 1,2- <i>cis</i> ^{a,b}	Yield ^c
Ribose					
1	34 R = H		38 R = D	<2:98	50%
2	8 R = Me		26 R = Me	98:<2	64%
3	9 R = Ph		27 R = Ph	98:<2	78%
Arabinose					
4	35 R = H		39 R = D	<2:98	62%
5	10 R = Me		28 R = Me	98:<2	83%
6	11 Ph		29 R = Ph	85:15	65%
Xylose					
7	36 R = H		40 R = D	15:85	40%
8	12 R = Me		30 R = Me	85:15	87%
9	13 R = Ph		31 R = Ph	75:25	79%
Lyxose					
10	37 R = H		41 R = D	<2:98	100%
11	16 R = Me		32 R = Me	98:<2	44%
12	17 R = Ph		33 R = Ph	98:<2	60%

^aRatio determined by ¹H NMR spectroscopy; stereochemistry was established using ²J coupling constants measured from HSQC-HECADE NMR spectra.⁷ ^bThe 1,2-*cis* addition of TES-D to aldoses affords the *cis* product, while addition of TES in ketose gives the *trans* product because of differing priorities of the anomeric substituents. ^cYield of isolated furanosides after column chromatography.

RESULTS AND DISCUSSION

The synthesis of the furanosyl lactols used in this study and the Lewis acid mediated reduction reactions are depicted in Scheme 2. The ribose-, arabinose-, and xylose-derived perbenzylated methyl and phenyl ketofuranose starting materials were prepared from the perbenzylated lactones. Ribonolactone **1**, arabinolactone **5**, and xylonolactone **6** were reacted with methyl lithium or phenyl lithium to yield the methyl and phenyl ketofuranoses that were directly used in the reduction step. Subjection of perbenzylated lyxonolactone **7** to methyl or phenyl lithium did not yield the desired ketofuranoses but only led to furan **14**, as the result of a double β -elimination sequence. Because furan formation could not be suppressed, we decided to generate the lyxose oxocarbenium ions in situ in the projected reduction reactions from their linear precursors **16** and **17**. These were synthesized from Weinreb amide **15** that was generated from lactone **7** using *N,O*-dimethylhydroxylamine together with trimethylaluminum, followed by capping of the alcohol function with triethylsilyl chloride (TES-Cl). Reaction of Weinreb amide **15** with methyl or phenyl lithium delivered the open chain ketones **16** and **17**.

The six ketofuranoses **8–13** and the two linear chain lyxose-derived ketones **16** and **17** were subjected to a Lewis acid mediated reduction protocol using triethylsilane as reducing agent and boron trifluoride diethyl etherate as Lewis acid in dichloromethane at -78 °C. The results of these reactions are summarized in Table 1, in combination with the results obtained in the experiments with the corresponding aldoses **34–37** (see Figure 2), in which furanosyl acetates were treated with TES-D and trimethylsilyl trifluoromethanesulfonate (TMSOTf).⁶ In all cases, preferentially the 1,2-*trans* C-furanosides were formed, corresponding to an attack of the hydride *cis* with respect to the substituent at C2. These results closely resemble those obtained for the aldoses **34–37**. In the case of ribose and lyxose, the reactions were completely

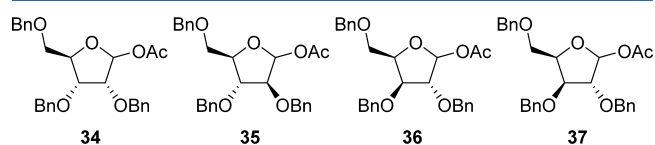


Figure 2. Reference aldose furanosyl donors used in our previous study.⁶

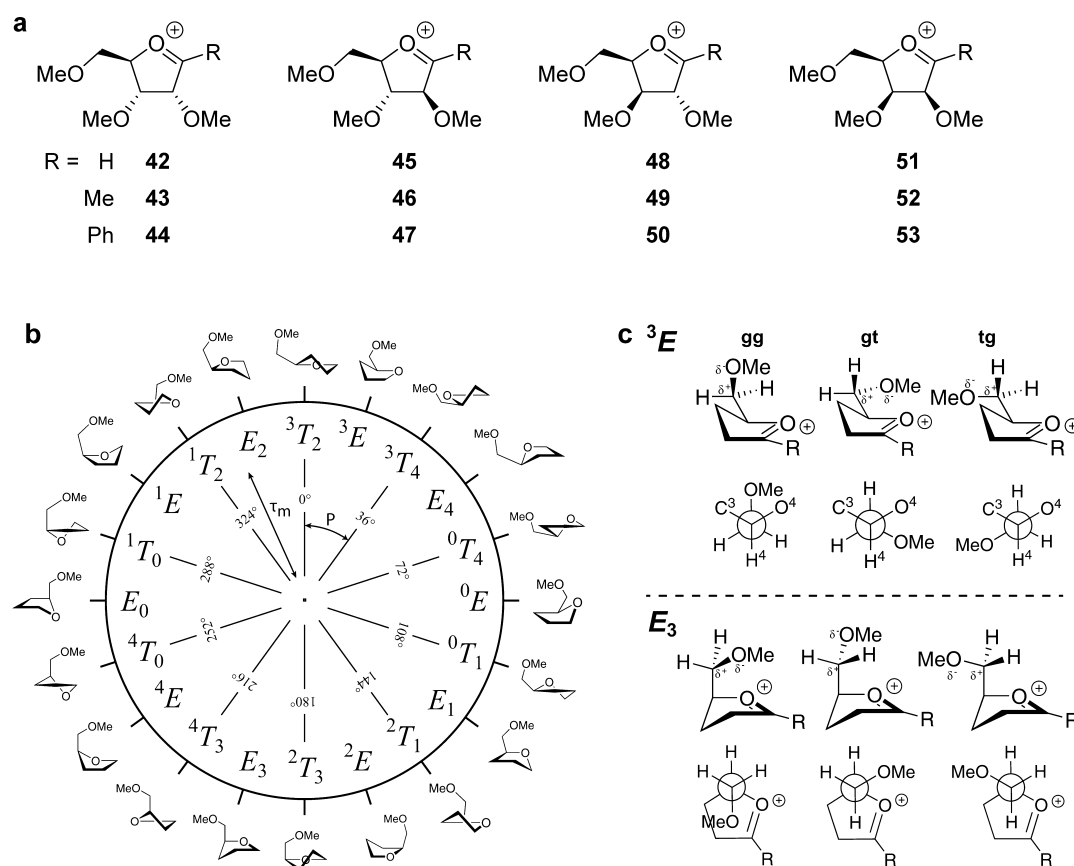


Figure 3. (a) Investigated furanosyl oxocarbenium ions. (b) Pseudorotational circle describing the conformational space that a five-membered ring can occupy. (c) Possible rotamers around the C4–C5 bond in the ³E (top) and E₃ (bottom) envelope conformers.

stereoselective and the products were obtained as a single diastereomer, independent of the substituent at the anomeric position (entries 1–3 and 10–12). In the arabinose series, both the aldose **35** and methyl ketofuranose **10** yielded a single product, whereas the reduction of phenyl ketofuranose **11** proceeded with a somewhat smaller stereoselectivity (entries 4–6). The *xylo*-aldofuranose **36** and *xylo*-methyl ketofuranose **12** yielded the 1,2-*cis* addition products with a similar preference,^{2b} where the phenyl ketofuranose **13** displayed the lowest stereoselectivity (entries 7–9).

In order to clarify the stereoselectivity observed in the reduction of the ketofuranoses and to assess the influence of the substituent (R = CH₃ or Ph) on the anomeric position on the intermediate oxocarbenium ions, the energy landscapes of the permethylated ketofuranosyl oxocarbenium ions **43**, **44**, **46**, **47**, **49**, **50**, **52**, and **53** (Figure 3a) were calculated. For this purpose, we used the free energy surface (FES) mapping method, as introduced by Rhoad and co-workers⁸ and adapted by us to interrogate aldofuranosyl oxocarbenium ions.⁶ In this method, the energy associated with the complete conformational space is calculated, and mapped on a circular graph, the pseudorotational circle (see Figure 3b).⁹ Each conformation is described by a phase angle (*P*) that defines the shape of the ring and by the puckering amplitude (τ_m) that indicates how far out of the median plane the outlying atoms are positioned.¹⁰ The energies of 81 fixed ring conformers were calculated with Gaussian 03,¹¹ employing the B3LYP density functional and the 6-311G** basis set, and these were corrected for the solvent CH₂Cl₂ using the polarizable continuum model function. Because rotation of the C4–C5 bond significantly influences

the stability of the furanosyl oxocarbenium ions,⁶ the FES of the oxocarbenium ions was scanned for the three individual *gg*, *gt*, and *tg* C4–C5 rotamers (Figure 3c). Thus, for each furanosyl oxocarbenium ion, 243 (3 × 81) conformers were optimized and their associated energies determined. For comparison, also the FES maps of the permethylated aldofuranosyl oxocarbenium ions **42**, **45**, **48**, and **51** are presented.⁶

Ribose. In Figure 4, the FES maps for the ribofuranosyl (**42**), methyl ribofuranosyl (**43**), and phenyl ribofuranosyl (**44**) oxocarbenium ions are depicted. In the columns from left to right, the *gg*, *gt*, *tg*, and the global lowest FES maps are displayed. The global FES map is composed by taking the absolute lowest energy of the *gg*, *gt*, and *tg* rotamers for a particular ring conformation and plotting these in a single map. The maps indicate that the ribofuranosyl E₃ oxocarbenium ion is highly preferred over the ³E conformer, independent of the nature of the anomeric substituent.¹² In the E₃ conformers, the C2 and C3 methoxy groups adopt a pseudoequatorial and pseudoaxial position, respectively, maximizing their stabilizing effect on the oxocarbenium ion. In all oxocarbenium ions (**42**–**44**), the C4–C5 *gg* rotamer is more stable than its *gt* counterpart, which in turn is preferred over the *tg* conformer. Small differences are present in the maps for the three anomeric substituents (R = H, Me, and Ph). The energy maps of the methyl furanosyl oxocarbenium ion conformers are somewhat steeper than the maps of its unsubstituted ion congener. The phenyl ribofuranosyl oxocarbenium ion maps, on the other hand, show a smaller energy difference between the ³E *gg* and E₃ *gg* conformer, but also in this case, the energy difference is

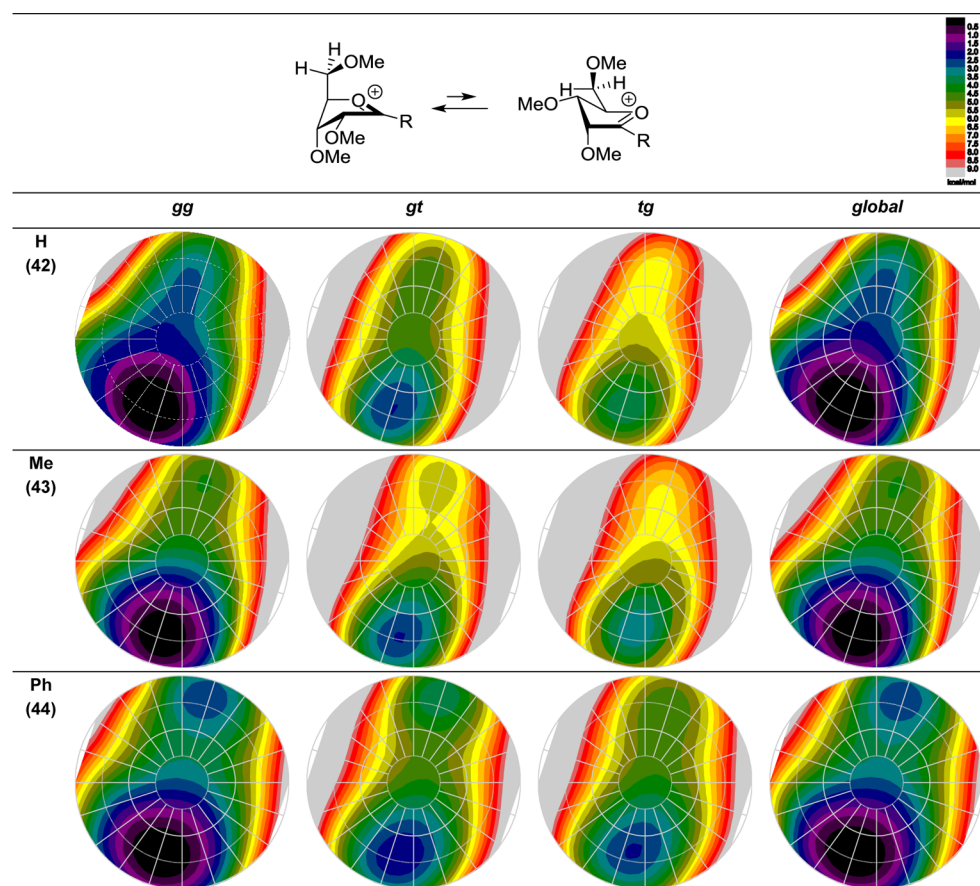


Figure 4. The *gg*, *gt*, *tg*, and global FES maps of the ribofuranosyl oxocarbenium ions 42–44.

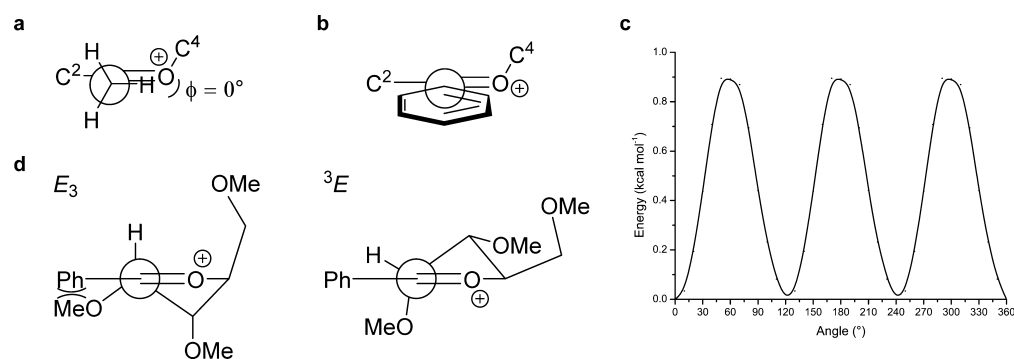


Figure 5. Conformation of the anomeric substituents relative to the oxocarbenium ion for (a) methyl and (b) phenyl. (c) Rotation energy profile of the anomeric methyl substituent for the ribofuranosyl oxocarbenium ion 43. (d) Steric interactions in two conformers of phenyl-substituted oxocarbenium ion 44.

sufficiently large ($\sim 2.7 \text{ kcal mol}^{-1}$) to account for the selectivity in the reaction ($98 < 2$, Table 1, entry 3).

A closer look at the structures associated with the energies in the FES maps of the methyl ketofuranosyl ion 43 reveals that the methyl substituent is placed in an eclipsed conformation with respect to the plane of the oxocarbenium ion [$\text{C}=\text{O}^+$] function (Figure 5a). To investigate the influence of the rotation of the methyl substituent around the C1–methyl bond, the energy profile associated with this rotation was calculated. As can be seen in Figure 5c, the eclipsed conformation is the most stable one, and the perpendicular structure ($\phi = 90^\circ$) that allows optimal hyperconjugative stabilization from a $\beta\text{-C-H}$ bond is $0.4 \text{ kcal mol}^{-1}$ higher in energy. This resembles the energy profile for the position of a

methyl substituent next to a carbonyl group.¹³ An analogous analysis for the phenyl ketofuranose reveals that the phenyl substituent is positioned parallel to the $\text{C}=\text{O}^+$ plane (Figure 5b), allowing effective conjugative stabilization of the positive charge. In the E_3 conformation, this planar constellation does lead to an unfavorable 1,3-allylic interaction between the phenyl ring and the substituent on C2 (Figure 5d). This allylic strain destabilizes the E_3 conformer and thereby decreases the energy difference with the 3E conformers. This, in combination with the conjugative stabilization by the phenyl substituent, leads to flattening of the FES maps for the phenyl ketofuranoses.

The FES maps for the nonsubstituted ($\text{R} = \text{H}$) and the methyl- and phenyl-substituted ribofuranosyl oxocarbenium ions 42–44 show that a single envelope is preferred in all three

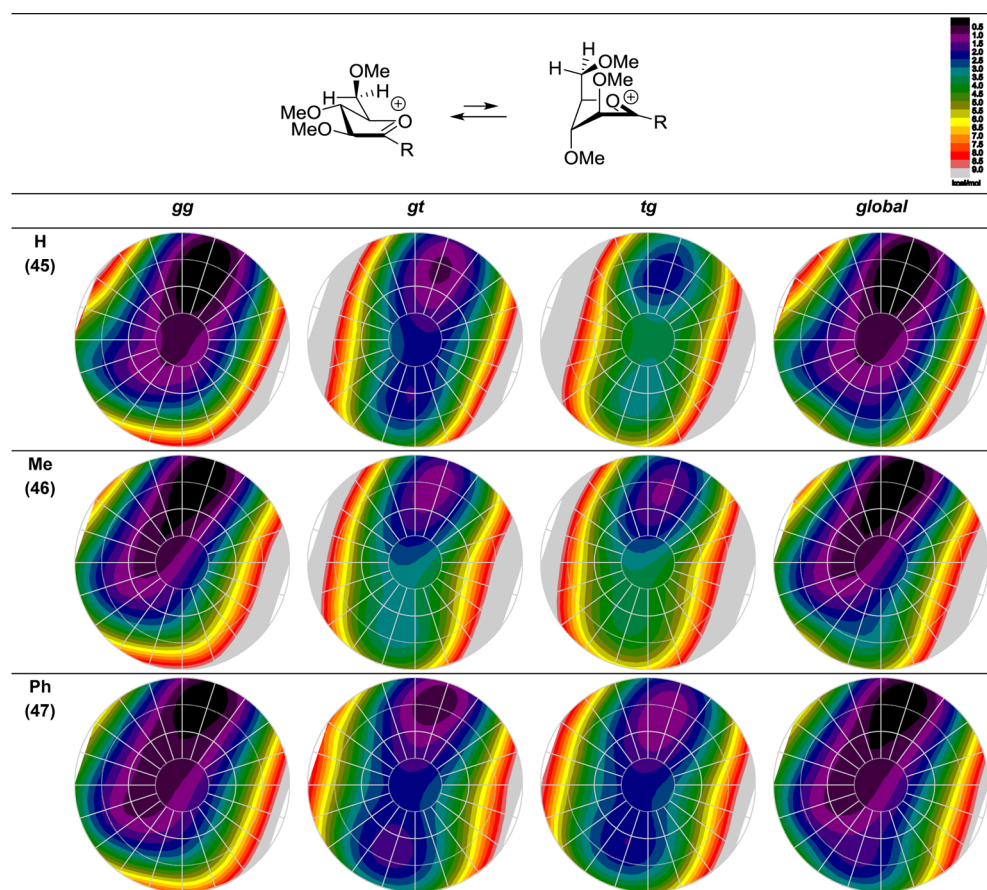


Figure 6. The *gg*, *gt*, *tg*, and global FES maps of the arabinofuranosyl oxocarbenium ions 45–47.

cases, that is, the E_3 conformer. Inside attack of the nucleophile (TES) on this conformer leads to the formation of 1,2-*cis* addition products, providing an explanation for the stereoselectivity observed in the reaction of **34**, **8**, and **9** (Table 1, entries 1–3).

Arabinose. The FES maps of the arabinofuranosyl oxocarbenium ions **45**, **46**, and **47** ($R = H, Me, \text{ and } Ph$) are displayed in Figure 6. The global FES maps indicate that all three ions preferentially adopt an 3E conformation. The individual C4–C5 rotamer maps reveal that the *gg* conformers are the most stable. The conformational preference of the arabinosyl oxocarbenium ions (**45**–**47**) is less profound than the preference of the corresponding *ribo*-oxocarbenium ions (**42**–**44**). This may be due to the fact that the C2 and C3 substituents cannot simultaneously adopt their most favorable orientation in either of the envelope structures. As is the case of the ribofuranosyl oxocarbenium ions, the FES maps for the methyl-substituted arabinofuranosyl ion **46** are somewhat steeper than for the aldose ion **45**, while the maps for the phenyl-substituted arabinofuranosyl ion **47** are somewhat less steep. The global FES maps of ions **45**–**47** do not show a distinct two conformer model; instead they show a gradual increase in energy for the conformers around the 3E – E_3 axis (18 – 198°). On the basis of the flattened FES of the phenyl ketose oxocarbenium ion **47**, one predicts an erosion of stereoselectivity in reactions involving this species. This is confirmed in the experiments: the arabino aldose and methyl ketofuranose both provide a single product upon reduction, whereas arabino phenyl ketofuranose gives an anomeric mixture

with the 1,2-*cis* addition product as major components (Table 1, entries 4–6) originating from a 3E oxocarbenium ion.

Xylose. The reductions of the xylofuranosides proceed with the least selectivity of the studied furanoses. The global FES maps of xylofuranose oxocarbenium ions **48**–**50** (Figure 7) show two energy minima, accounting for the formation of two anomers in the experiments. The major conformer of ions **49** and **50** is the *gg* E_3 envelope, where the minor 3E conformer places the C5 methoxy group in a *gt* position. For the aldose ion **48**, the lowest energy conformation is 4T_3 , a structure that slightly deviates from the E_3 conformer. This conformation optimally positions the C5-OMe over the furanosyl ring, providing the most stabilization. In the ketoxylofuranosyl FES maps, this effect is less pronounced. As in the case of the ribo and arabino ions, the energy difference between the E_3 and 3E conformers of the methyl ketofuranosyl ion **49** is somewhat larger than the difference observed for aldofuranose ion **48** and somewhat smaller for the phenyl furanosyl oxocarbenium ion **50**. The larger energy difference between the E_3 and 3E methyl xylofuranosyl oxocarbenium ions compared to the aldose case (Table 1, entries 7–9) is not reflected in the experimental results. The phenyl ketose ion **50** shows a larger preference toward the 3E envelope than the methyl ketofuranose ion **49**. It still maintains the E_3 as the major conformer, but with a smaller energy difference between the two envelopes. The shallower FES map for the phenyl xylofuranosyl oxocarbenium ion **50** accounts for the lower stereoselectivity observed in the reduction of phenyl ketose **13** (Table 1, entry 9).

Lyxose. In Figure 8, the FES maps for the lyxofuranosyl oxocarbenium ions **51**–**53** are displayed. We previously found

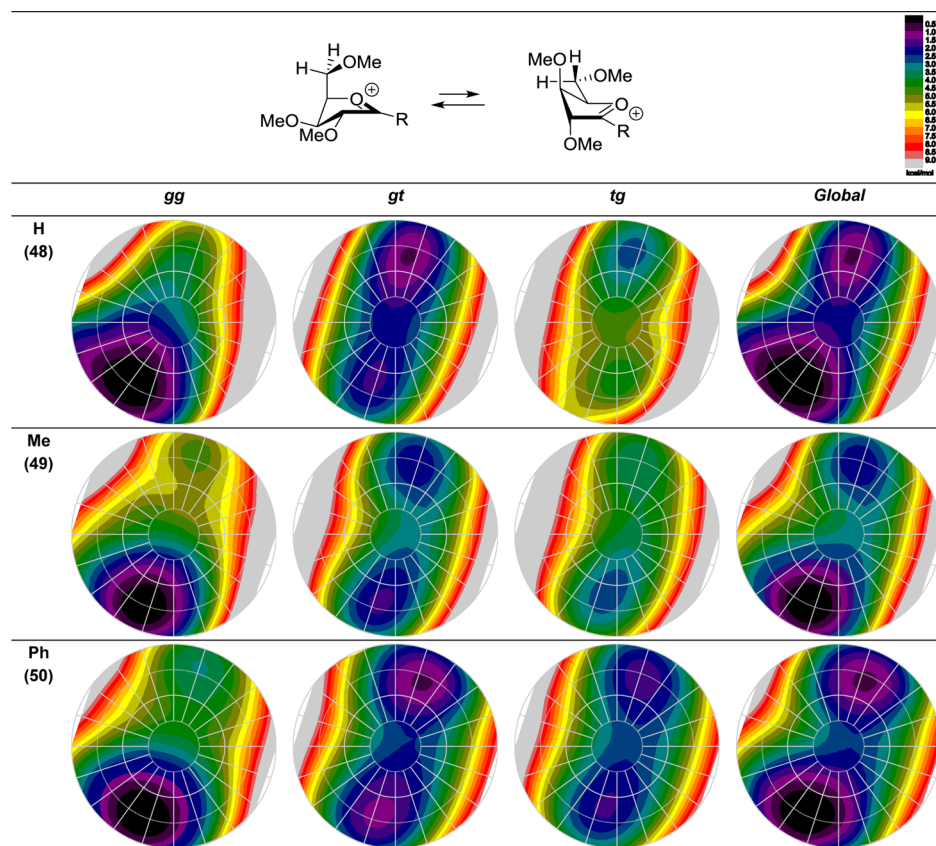


Figure 7. The *gg*, *gt*, *tg*, and global FES maps of the xylofuranosyl oxocarbenium ions 48–50.

a strong preference for the 3E envelope of lyxofuranosyl oxocarbenium ion 51 ($R = H$) and the associated remarkable stereoselectivity in additions to this intermediate (*cis* with respect to *all* ring substituents).⁶ This strong conformational preference is maintained in the ketofuranosyl oxocarbenium ions 52 and 53, as shown in the global FES maps. In all three 3E oxocarbenium ions, the C2 substituent is in the preferred pseudo-equatorial position and the C3 substituent is in a pseudo-axial position, allowing stabilization of the positive charge at the anomeric position. The FES map of the individual C4–C5 rotamer shows a preference for C5 *gt*, avoiding a sterically and electronically unfavorable interaction with the axial C3 substituent. Inside attack of the nucleophile on the lyxofuranosyl 3E oxocarbenium ions leads to the 1,2-*cis* addition product in both the aldose and ketoses.

CONCLUSION

Substitution reactions at the anomeric center of aldofuranoses as well as ketofuranoses proceed with remarkable stereoselectivity to provide 1,2-*cis* addition products, independent of the substitution pattern on the carbohydrate ring. The stereoselectivity presumably is the result of a sequence of reactions in which the most stable intermediate oxocarbenium ion conformer is attacked from the inside by the nucleophile in the product-forming step. Mapping of the FES of the complete conformational space of the oxocarbenium ions involved substantiates this mechanistic model: the calculated energy differences between the envelopes of the differently configured aldofuranoside and ketofuranoside ions parallel the observed stereoselectivity in the reactions. Overall, significant similarities exist between the FES maps for the ketoses studied here and

those previously described for the aldoses. An anomeric methyl substituent in the ketose ions makes the preference for one of the two envelopes more distinct than in the case of the aldose ions, and an anomeric phenyl substituent, on the other hand, leads to smaller energy differences between the envelopes. The latter effect can be partially attributed to the destabilizing 1,3-allylic strain between the anomeric phenyl ring positioned parallel to the $C=O^+$ plane and the pseudo-equatorial C2 substituent. Also, the conjugative stabilization of the oxocarbenium ion by the phenyl ring can lead to a smaller energy difference between the different oxocarbenium ion conformers. The calculated differences in energy between the various oxocarbenium ion envelopes provide a reliable prediction for the stereoselectivity of substitution reactions involving addition to these intermediates. It appears that in the addition reactions studied here a Curtin–Hammett kinetic scenario in which a reaction on the higher energy intermediate proceeds via a lower overall transition state, thereby providing the prevalent reaction path, does not play a major role. Given the fact that the oxocarbenium ion intermediates are high-energy species, the transition states of the reactions proceeding through these intermediates will be early and therefore resemble the structures of the oxocarbenium ions. The relative product ratios observed for the additions to the phenyl ketofuranosides deviate most from the product ratios predicted from the FES maps. The phenyl ketofuranosyl oxocarbenium ions are the most stable intermediates of the three oxocarbenium ion types studied, and therefore, the transition states for reactions taking place on these ions will be the latest of the series, departing most from the ground-state oxocarbenium ion structure. Here, other factors, such as steric

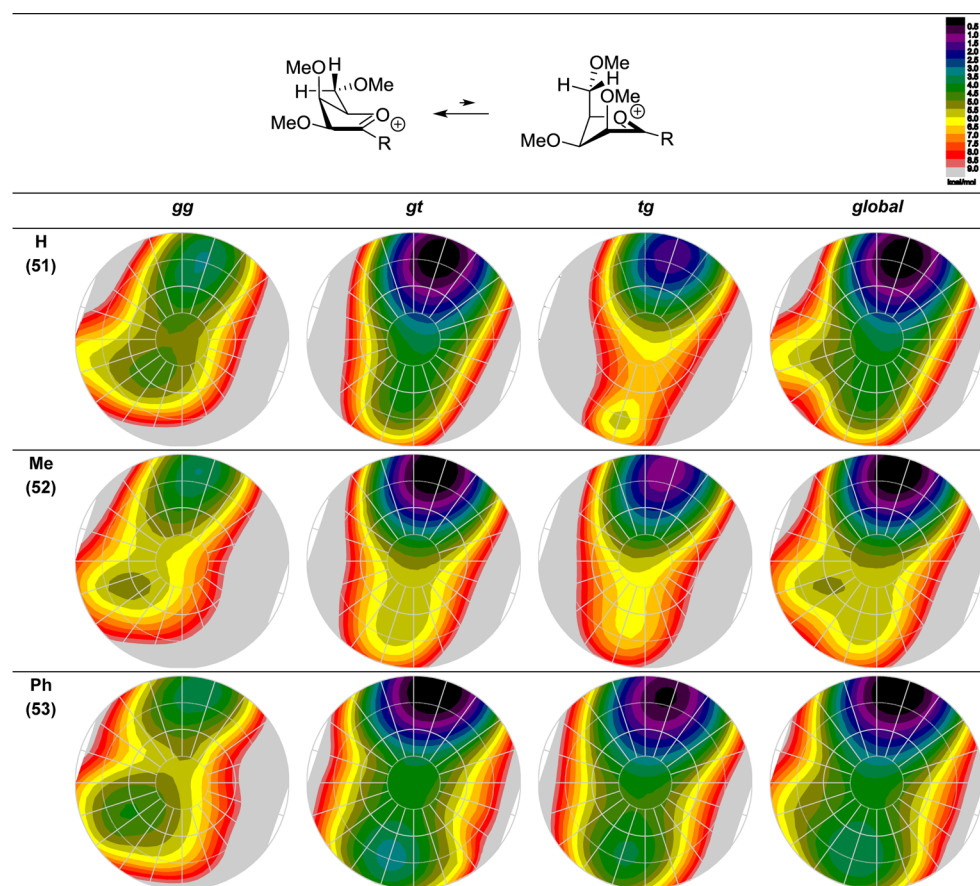


Figure 8. The *gg*, *gt*, *tg*, and global FES maps of the lyxofuranosyl oxocarbenium ions 51–53.

interactions between the nucleophile and the electrophile, will become more important, opening the way for a Curtin–Hammett scenario described above. In all, the Lewis acid mediated reduction of ketofuranosides provides efficient access to a range of C-glycosides with predictable stereochemistry.

EXPERIMENTAL SECTION

In all calculations, methyl ethers were used because of their reduced calculation costs over benzyl ethers. All calculations were performed with density functional theory ab initio calculations with the B3LYP model. The starting conformer for the FES was optimized by starting from a conformer distribution search option included in the Spartan 04¹⁴ program in the gas phase with the 6-31G* basis set. All generated geometries were optimized with Gaussian 03¹¹ at 6-311G***, and their zero-point energy (ZPE) corrections were calculated and further optimized with an incorporated polarizable continuum model to correct for solvation in dichloromethane. The geometry with the lowest ZPE-corrected, solvated free energy was selected as the starting point for the FES. Two dihedral angles of the five-membered ring were constrained, namely, C4–O4–C1–C2 (τ_0 , θ_3) and C1–C2–C3–C4 (τ_2 , θ_0), with angles from -40 to 40° over nine steps (10° per step), giving a total of 81 conformers and dictating the entire pseudorotational space within a maximum amplitude (τ_m) of 40° . All other internal coordinates were unconstrained. The geometries were optimized, and their ZPE was calculated and corrected for solvation with Gaussian 03 at 6-311G** as above. The FES was visualized as a polar contour plot through the Origin 8.5 graphing software by putting the phase angle (P) as θ , the amplitude (τ_m) at r , and the energy corrected for ZPE and optimized in solvent at the Z-axis. To interrogate all rotamers of the C5 substituent, the starting conformer was modified by rotating the O4–C4–C5–O5 dihedral angle to each of the three staggered configurations (*gauche-gauche* = -65° , *gauche-*

trans = 65° , *trans-gauche* = 175°) and then generating the FES through the above-mentioned method, generating a total of 243 optimized geometries. These three FES maps were graphed individually and in a combined plot by comparing the corrected free energies and, for each point, selecting the geometry of lowest energy from the three entities.

2,3,5-Tri-O-benzyl-D-ribo-1,4-lactone (1). 2,3,5-Tri-O-benzyl-D-ribofuranose (10.2 mmol) was dissolved in dimethylsulfoxide (DMSO) (15 mL, 211 mmol) and cooled to 0°C , and acetic anhydride (10 mL, 106 mmol) was added and the mixture stirred overnight. The reaction was poured onto ice water and extracted with diethyl ether (3 \times). The combined organic layers were washed with H₂O (3 \times) and brine, dried over MgSO₄, filtered, and concentrated under reduced pressure. The residue was purified by silica gel column chromatography (30% Et₂O/pentane), yielding the title compound (3.82 g, 9.1 mmol, 89%): $R_f = 0.30$ (30/70 Et₂O/petroleum ether); ¹H NMR (400 MHz, CDCl₃) δ 7.39–7.26 (m, 13H, CH_{Ar} Bn), 7.16 (dd, $J = 7.3, 2.2$ Hz, 2H, CH_{Ar} Bn), 4.94 (d, $J = 12.0$ Hz, 1H, CHH Bn), 4.74 (d, $J = 12.0$ Hz, 1H, CHH Bn), 4.69 (d, $J = 11.8$ Hz, 1H, CHH Bn), 4.56–4.52 (m, 2H, CHH Bn, C-4), 4.49 (d, $J = 11.9$ Hz, 1H, CHH Bn), 4.44–4.36 (m, 2H, CHH Bn, C-2), 4.09 (dd, $J = 5.6, 2.0$ Hz, 1H, C-3), 3.66 (dd, $J = 11.0, 2.9$ Hz, 1H, C-5a), 3.55 (dd, $J = 11.0, 2.7$ Hz, 1H, C-5b). ¹³C NMR (101 MHz, CDCl₃) δ 173.8 (C=O), 137.4, 137.2, 137.1 (C_q Bn), 128.7, 128.6, 128.6, 128.4, 128.2, 128.2, 128.1, 127.7 (CH_{Ar} Bn), 81.9 (C-4), 75.5 (C-3), 73.8 (C-2), 73.8, 72.8, 72.5 (3 \times CH₂ Bn), 68.9 (C-5); $[\alpha]_D^{20} = 73$ ($c = 1$, CHCl₃); IR (neat) 602, 615, 652, 692, 733, 764, 781, 824, 854, 891, 908, 934, 957, 974, 995, 1011, 1022, 1084, 1098, 1155, 1182, 1215, 1233, 1246, 1333, 1362, 1400, 1454, 1497, 1773, 2874, 2909, 3030; HRMS (ESI) $[M + H]^+$ calcd for C₂₆H₂₆O₅ 419.18530, found 419.18553.

1-C-(5'-(2',3'-Di-*tert*-butoxy)pyrimidine)-2,3,5-tri-O-benzyl-D-ribofuranose (3). To a stirred and cooled (-78°C) solution of, with toluene coevaporated (3 \times), 5-bromo-2,4-di-*tert*-butoxypyrimi-

dine¹⁵ (2.4 g, 8 mmol) in anhydrous tetrahydrofuran (THF) (40 mL) was added a solution of *n*-BuLi (5.5 mL, 8.8 mmol, 1.6 M in hexanes). After 20 min at -78°C , with toluene coevaporated (3 \times), 2,3,5-tri-*O*-benzyl-*D*-arabino-1,4-lactone (**5**, 5.0 g, 11.8 mmol) in anhydrous THF (40 mL) was added dropwise over 45 min. The mixture was allowed to slowly warm to -55°C over a period of 4 h after which thin layer chromatography (TLC) indicated complete reaction. The reaction mixture was cooled to -78°C and was quenched by the addition of NaH_2PO_4 (8 mL, 20% aq). The reaction mixture was allowed to warm to room temperature, diluted with EtOAc, and washed with H_2O (2 \times) and brine, dried over Na_2SO_4 , filtered, and concentrated under reduced pressure. Silica gel purification (5–15% EtOAc/toluene) yielded the title compound (2.98 g, 4.6 mmol, 58%), which was used directly in the next step.

2',3',5'-Tri-*O*-benzyl-pseudouridine (4). To a stirred and cooled (-78°C) solution of, with toluene coevaporated (3 \times), 1-*C*-(5'-(2',3'-di-*tert*-butoxy)pyrimidine)-2,3,5-tri-*O*-benzyl-*D*-ribofuranose (**3**, 2.84 g, 4.4 mmol) in anhydrous dichloromethane (DCM) (15 mL) were added triethylsilane (0.95 mL, 5.9 mmol) and $\text{BF}_3\cdot\text{Et}_2\text{O}$ (1.56 mL, 11 mmol). The reaction was allowed to slowly warm to 10°C and stirred overnight at this temperature. The reaction mixture was cooled to -5°C before TFA (15 mL) was added. The solution was stirred for 90 min, poured on ice water, and extracted with DCM. The organic layer was washed with saturated aq NaHCO_3 , H_2O (3 \times) and brine, dried over Na_2SO_4 , filtered, and concentrated under reduced pressure. The residue was purified by silica gel column chromatography (5–15% acetone/DCM), yielding 5-(2,3,5-tri-*O*-benzyl- β -*D*-ribofuranosyl)uracil (1.53 g, 3.0 mmol, 68% yield over 2 steps) as a single diastereomer: $R_f = 0.15$ (10/90 acetone/DCM); $^1\text{H NMR}$ (400 MHz, CDCl_3) δ 9.63 (s, 1H, NH-3), 8.77 (d, $J = 5.6$ Hz, 1H, NH-1), 7.59 (d, $J = 5.9$ Hz, 1H, C-6), 7.50–7.38 (m, 2H, 2 \times CH_{Ar} Bn), 7.37–7.14 (m, 13H, CH_{Ar} Bn), 5.04 (s, 1H, C-1'), 4.85 (d, $J = 12.3$ Hz, 1H, CHH Bn), 4.74 (d, $J = 12.3$ Hz, 1H, CHH Bn), 4.51–4.45 (m, 2H, 2 \times CHH Bn), 4.42 (d, $J = 11.4$ Hz, 1H, CHH Bn), 4.34–4.19 (m, 2H, CHH Bn, C-4'), 4.02 (d, $J = 4.6$ Hz, 1H, C-2'), 3.95 (dd, $J = 8.6, 4.6$ Hz, 1H, C-3'), 3.87 (dd, $J = 10.7, 2.2$ Hz, 1H, C-5'a), 3.63 (dd, $J = 10.8, 2.7$ Hz, 1H, C-5'b); $^{13}\text{C NMR}$ (101 MHz, CDCl_3) δ 163.0 (C-4), 152.0 (C-2), 139.1 (C-5), 138.2, 138.2, 137.8 (C_q Bn), 128.6, 128.5, 128.5, 128.4, 128.0, 127.9, 127.8, 127.8 (CH_{Ar} Bn), 113.1 (C-6), 79.4 (C-4'), 78.6 (C-2'), 78.3 (C-1'), 75.7 (C-3'), 73.3, 72.0, 71.3 (CH_2 Bn), 68.7 (C-5'); IR (neat) 694, 731, 818, 1001, 1026, 1040, 1074, 1084, 1121, 1204, 1356, 1427, 1452, 1495, 1661, 1703, 2860, 2913; $[\alpha]_{\text{D}}^{20} = 149.7$ ($c = 1.1$, CHCl_3); HRMS (ESI) $[\text{M} + \text{H}^+]$ calcd for $\text{C}_{30}\text{H}_{30}\text{N}_2\text{O}_6$ 515.21766, found 515.21771.

1-Methyl-2,3,5-tri-*O*-benzyl-*D*-ribofuranose (8). To a stirred and cooled (-78°C) solution of, with toluene coevaporated (3 \times), 2,3,5-tri-*O*-benzyl-*D*-ribo-1,4-lactone (**6**, 0.9 mmol, 380 mg) in anhydrous THF (3 mL) was added dropwise (20 min) methyl lithium (0.69 mL, 1.1 mmol, 1.6 M in hexanes). After 2 h, an additional 0.2 mmol of methyl lithium (0.125 mmol) was added. The reaction was quenched by the addition of saturated aq NH_4Cl (0.8 mL), diluted with EtOAc, and allowed to warm to room temperature. The organic layer was washed with H_2O (2 \times) and brine, dried over MgSO_4 , filtered, and concentrated under reduced pressure. Silica gel purification (40/60 Et_2O /petroleum ether) allowed removal of any unreacted components and yielded the title compound (310 mg, 0.7 mmol, 77%), which was used directly in the next step: $R_f = 0.15$ (30/70 Et_2O /petroleum ether).

β -1-Methyl-1-deoxy-2,3,5-tri-*O*-benzyl-*D*-ribofuranose (26). To a stirred and cooled (-78°C) solution of, with toluene coevaporated (3 \times), 1-methyl-2,3,5-tri-*O*-benzyl-*D*-ribofuranose (**8**, 220 mg, 0.5 mmol) in anhydrous DCM (5 mL) were added triethylsilane (242 μL , 1.5 mmol) and $\text{BF}_3\cdot\text{Et}_2\text{O}$ (380 μL , 3.0 mmol). The reaction was stirred at -78°C for 1.5 h, after which TLC analysis indicated complete conversion. The reaction mixture was quenched by addition of saturated aq NaHCO_3 (1 mL). The reaction mixture was diluted with EtOAc and washed with saturated aq NaHCO_3 (2 \times), H_2O , and brine, dried over MgSO_4 , filtered, and concentrated under reduced pressure. The residue was purified by silica gel column chromatography (10% EtOAc/petroleum ether) and yielded β -1-

methyl-1-deoxy-2,3,5-tri-*O*-benzyl-*D*-ribofuranose (140 mg, 0.32 mmol, 64%) as a single diastereomer: $R_f = 0.85$ (20/80 EtOAc/petroleum ether); $^1\text{H NMR}$ (400 MHz, CDCl_3) δ 7.35–7.23 (m, 15H, CH_{Ar} Bn), 4.60 (d, $J = 11.9$ Hz, 1H, CHH Bn), 4.55 (s, 2H, CH_2 Bn), 4.55 (d, $J = 12.1$ Hz, 1H, CHH Bn), 4.50 (d, $J = 12.0$ Hz, 1H, CHH Bn), 4.48 (d, $J = 11.9$ Hz, 1H, CHH Bn), 4.19–4.14 (m, 1H, C-4), 4.13–4.06 (m, 1H, C-1), 3.87 (dd, $J = 5.3, 4.3$ Hz, 1H, C-3), 3.49 (d, $J = 4.5$ Hz, 2H, C-5), 3.46 (dd, $J = 6.7, 5.7$ Hz, 1H, C-2), 1.25 (d, $J = 6.3$ Hz, 3H, CH_3); $^{13}\text{C NMR}$ (101 MHz, CDCl_3) δ 138.2, 138.0, 138.0 (C_q Bn), 128.4, 128.4, 128.4, 128.2, 127.9, 127.8, 127.7, 127.6 (CH_{Ar} Bn), 82.6 (C-2), 81.7 (C-4), 77.5 (C-3), 76.9 (C-1), 73.5, 72.1, 71.8 (3 \times CH_2 Bn), 70.7 (C-5), 19.1 (CH_3); $[\alpha]_{\text{D}}^{20} = -10$ ($c = 1.1$, CHCl_3); IR (neat) 697, 736, 1027, 1097, 1454, 1721, 2872; HRMS (ESI) $[\text{M} + \text{Na}]^+$ calcd for $\text{C}_{27}\text{H}_{30}\text{O}_4$ 441.20363, found 441.20330.

1-Phenyl-2,3,5-tri-*O*-benzyl-*D*-ribofuranose (9). To a stirred and cooled (-78°C) solution of bromobenzene (115 μL , 1.1 mmol) in anhydrous THF (4 mL) was added *n*-BuLi (0.74 mL, 1.2 mmol, 1.6 M in hexanes). After 20 min at -78°C , a solution of, with toluene coevaporated (3 \times), 2,3,5-tri-*O*-benzyl-*D*-ribo-1,4-lactone (**1**, 382 mg, 0.9 mmol) in anhydrous THF (4 mL) was added dropwise. After 2 h, the reaction mixture was quenched by the addition of saturated aq NH_4Cl (4 mL) at -78°C . The reaction mixture was allowed to warm to room temperature, diluted with EtOAc, washed with H_2O (2 \times) and brine, dried over MgSO_4 , filtered, and concentrated under reduced pressure. Silica gel purification (20–30% Et_2O /petroleum ether) allowed removal of any unreacted components and yielded the title compound (218 mg, 0.44 mmol, 48%) which was used directly in the next step: $R_f = 0.30$ (30/70 Et_2O /petroleum ether).

β -1-Phenyl-1-deoxy-2,3,5-tri-*O*-benzyl-*D*-ribofuranose (27). To a stirred and cooled (-78°C) solution of, with toluene coevaporated (3 \times), 1-phenyl-2,3,5-tri-*O*-benzyl-*D*-ribofuranose (**9**, 200 mg, 0.4 mmol) in anhydrous DCM (6 mL) were added triethylsilane (192 μL , 1.2 mmol) and $\text{BF}_3\cdot\text{Et}_2\text{O}$ (303 μL , 2.4 mmol). The reaction was stirred at -78°C for 1 h, after which the reaction was quenched by addition of saturated aq NaHCO_3 (6 mL). The reaction mixture was diluted with EtOAc and washed with saturated aq NaHCO_3 (2 \times), H_2O , and brine, dried over MgSO_4 , filtered, and concentrated under reduced pressure. The residue was purified by silica gel column chromatography (20% Et_2O /petroleum ether) and yielded β -1-phenyl-1-deoxy-2,3,5-tri-*O*-benzyl-*D*-ribofuranose (150 mg, 0.31 mmol, 78%) as a single diastereomer: $R_f = 0.60$ (30/70 Et_2O /petroleum ether); $^1\text{H NMR}$ (400 MHz, CDCl_3) δ 7.42–7.37 (m, 3H, CH_{Ar} Ph), 7.37–7.22 (m, 15H, CH_{Ar} Bn), 7.21–7.15 (m, 2H, CH_{Ar} Ph), 5.03 (d, $J = 6.6$ Hz, 1H, C-1), 4.61 (d, $J = 12.0$ Hz, 1H, CHH Bn), 4.60 (d, $J = 12.4$ Hz, 1H, CHH Bn), 4.59–4.55 (m, 1H, CHH Bn), 4.55 (d, $J = 11.9$ Hz, 1H, CHH Bn), 4.49 (d, $J = 12.6$ Hz, 1H, CHH Bn), 4.46 (d, $J = 12.9$ Hz, 1H, CHH Bn), 4.38–4.32 (m, 1H, C-4), 4.01 (dd, $J = 4.9, 4.4$ Hz, 1H, C-3), 3.81 (dd, $J = 6.5, 5.3$ Hz, 1H, C-2), 3.68 (dd, $J = 10.4, 4.2$ Hz, 1H, C-5a), 3.63 (dd, $J = 10.4, 4.0$ Hz, 1H, C-5b); $^{13}\text{C NMR}$ (101 MHz, CDCl_3) δ 140.5 (C_q Ph), 138.3, 138.0, 137.9 (C_q Bn), 128.5, 128.4, 128.4, 128.2, 127.9, 127.9, 127.8, 127.8, 127.7, 126.4 (CH_{Ar} Ph, CH_{Ar} Bn), 83.8 (C-2), 82.8 (C-1), 81.8 (C-4), 77.6 (C-3), 73.6, 72.3, 72.0 (CH_2 Bn), 70.5 (C-5); $[\alpha]_{\text{D}}^{20} = -18.2$ ($c = 1$, CHCl_3); IR (neat) 696, 730, 1010, 1051, 1106, 1144, 1367, 1454, 1496, 2358, 2870; HRMS (ESI) $[\text{M} + \text{Na}]^+$ calcd for $\text{C}_{32}\text{H}_{32}\text{O}_4$ 503.21928, found 503.21884.

2,3,5-Tri-*O*-benzyl-*D*-arabino-1,4-lactone (5). 2,3,5-Tri-*O*-benzyl-*D*-arabinofuranose (1.0 g, 2.4 mmol) was dissolved in DMSO (18.5 mL, 262 mmol); acetic anhydride (12.5 mL, 133 mmol) was added, and the reaction mixture was stirred for 4 days. The mixture was poured onto ice water and extracted with Et_2O . The organic layer was washed with H_2O (2 \times) and brine, dried over Na_2SO_4 , and concentrated under reduced pressure. The residue was crystallized from methanol, yielding the title compound (729 mg, 1.7 mmol, 73%): $R_f = 0.85$ (25/75 EtOAc/pentane); $^1\text{H NMR}$ (400 MHz, CDCl_3) δ 7.44–7.25 (m, 13H, CH_{Ar} Bn), 7.25–7.18 (m, 2H, CH_{Ar} Bn), 5.06 (d, $J = 11.6$ Hz, 1H, CHH Bn), 4.77 (d, $J = 11.6$ Hz, 1H, CHH Bn), 4.63 (d, $J = 11.6$ Hz, 1H, CHH Bn), 4.58–4.46 (m, 3H, 3 \times CHH Bn), 4.38–4.29 (m, 3H, C-2, C-3, C-4), 3.70 (dd, $J = 11.4, 2.3$ Hz, 1H, C-5a), 3.60–3.54 (m, 1H, C-5b); $^{13}\text{C NMR}$ (101 MHz, CDCl_3) δ 172.6

(C=O-1), 137.6, 137.2, 136.9 (C_q Bn), 128.7, 128.6, 128.6, 128.6, 128.3, 128.2, 128.0, 128.0, 127.9 (CH_{Ar} Bn), 79.3, 79.2, 78.9 (C-2, C-3, C-4), 73.6, 72.8, 72.6 (CH₂ Bn), 68.0 (C-5); [α]_D²⁰ = 6 (*c* = 1, CHCl₃); IR (neat) 633, 644, 962, 731, 804, 872, 903, 949, 988, 997, 1016, 1028, 1038, 1049, 1070, 1086, 1113, 1130, 1146, 1180, 1227, 1265, 1321, 1369, 1452, 1495, 1778, 2866, 2911, 3030; HRMS (ESI) [M + H⁺] calcd for C₂₆H₂₆O₅ 419.18530, found 419.18551.

1-Methyl-2,3,5-tri-O-benzyl-D-arabinofuranose (10). To a stirred and cooled (−78 °C) solution of, with toluene coevaporated (3×), 2,3,5-tri-O-benzyl-D-arabino-1,4-lactone (**5**, 418 mg, 1 mmol) in anhydrous THF (4 mL) was added methyl lithium (0.69 mL, 1.1 mmol, 1.6 M in Et₂O). After 6 h, the reaction was quenched by the addition of saturated aq NH₄Cl (4 mL), diluted with EtOAc, and allowed to warm to room temperature. The layers were separated, and the aqueous layer was extracted twice with EtOAc. The combined organic layers were washed with brine, dried over MgSO₄, filtered, and concentrated under reduced pressure. Silica gel purification (15–25% EtOAc/petroleum ether) allowed removal of any unreacted components and yielded the title compound as a colorless oil (386 mg, 0.87 mmol, 86%) which was used directly in the next step: *R*_f = 0.30 (25/75 EtOAc/petroleum ether).

α -1-Methyl-1-deoxy-2,3,5-tri-O-benzyl-D-arabinofuranose (28). To a stirred and cooled (−78 °C) solution of, with toluene coevaporated (3×), 1-methyl-2,3,5-tri-O-benzyl-D-arabinofuranose (**10**, 132 mg, 0.30 mmol) in anhydrous DCM (4.3 mL) were added triethylsilane (63 μ L, 0.40 mmol) and BF₃·Et₂O (50 μ L, 0.4 mmol). The reaction was stirred at −78 °C for 3 days at which TLC indicated complete conversion. The reaction mixture was quenched by addition of saturated aq NaHCO₃ (4 mL). The reaction mixture was extracted with EtOAc (3×), and the combined organic layers were washed with H₂O and brine, dried over MgSO₄, filtered, and concentrated under reduced pressure. The residue was purified by silica gel column chromatography (8–10% EtOAc/petroleum ether) and yielded α -1-methyl-1-deoxy-2,3,5-tri-O-benzyl-D-arabinofuranose (106 mg, 0.30 mmol, 83%) as a single diastereomer: *R*_f = 0.90 (25/75 EtOAc/petroleum ether); ¹H NMR (400 MHz, CDCl₃) δ 7.35–7.23 (m, 15H, CH_{Ar} Bn), 4.59–4.48 (m, 5H, 5× CHH Bn), 4.49 (d, *J* = 11.9 Hz, 1H, CHH Bn), 4.25–4.19 (m, 1H, C-4), 4.17–4.09 (m, 1H, C-1), 4.02 (t, *J* = 3.7 Hz, 1H, C-3), 3.76 (dd, *J* = 5.0, 3.3 Hz, 1H, C-2), 3.58 (dd, *J* = 9.9, 5.8 Hz, 1H, C-5a), 3.53 (dd, *J* = 10.0, 5.7 Hz, 1H, C-5b), 1.31 (d, *J* = 6.4 Hz, 3H, CH₃); ¹³C NMR (101 MHz, CDCl₃) δ 138.2, 138.0 (C_q Bn), 128.6, 128.5, 128.5, 127.9, 127.9, 127.8, 127.8, 127.7 (CH_{Ar} Bn), 89.4 (C-2), 85.6 (C-3), 81.2 (C-4), 78.3 (C-1), 73.5, 72.0, 72.0 (3× CH₂ Bn), 70.5 (C-5), 19.3 (CH₃); [α]_D²⁰ = 11.9 (*c* = 1.1, CHCl₃); IR (neat) 696, 734, 1028, 1092, 1722, 2864; HRMS (ESI) [M + H⁺] calcd for C₂₇H₃₀O₄ 419.22169, found 419.22165.

1-Phenyl-2,3,5-tri-O-benzyl-D-arabinofuranose (11). To a stirred and cooled (−78 °C) solution of phenyl bromide (115 μ L, 1.1 mmol) in anhydrous THF (1.5 mL) was added *n*-BuLi (0.74 mL, 1.1 mmol, 1.6 M in hexanes). After 20 min at −78 °C, with toluene coevaporated (3×), 2,3,5-tri-O-benzyl-D-arabino-1,4-lactone (**5**, 420 mg, 1 mmol) in anhydrous THF (1.5 mL) was added dropwise. After 1 h, the reaction was quenched by the addition of saturated aq NH₄Cl (0.5 mL) at −78 °C. The reaction mixture was allowed to warm to room temperature, diluted with EtOAc, and washed with H₂O and brine, dried over MgSO₄, filtered, and concentrated under reduced pressure. Silica gel purification (20% Et₂O/petroleum ether) allowed removal of any unreacted components and yielded the title compound (348 mg, 0.7 mmol, 70%) which was used directly in the next step: *R*_f = 0.70 (20/80 Et₂O/petroleum ether).

α/β -1-Phenyl-1-deoxy-2,3,5-tri-O-benzyl-D-arabinofuranose (29). To a stirred and cooled (−78 °C) solution of, with toluene coevaporated (3×), 1-phenyl-2,3,5-tri-O-benzyl-D-arabinofuranose (**11**, 275 mg, 0.55 mmol) in anhydrous DCM (8 mL) were added triethylsilane (233 μ L, 1.46 mmol) and BF₃·Et₂O (400 μ L, 3.2 mmol). The reaction was stirred at −78 °C for 1.5 h at which TLC analysis showed near complete conversion. The reaction was quenched by addition of saturated aq NaHCO₃ (1 mL). The reaction mixture was diluted with EtOAc and washed with saturated aq NaHCO₃ (2×), H₂O, and brine, dried over MgSO₄, filtered, and concentrated under

reduced pressure. The residue was purified by silica gel column chromatography (15% EtOAc/petroleum ether), yielding an anomeric mixture (α/β = 85:15) of α/β -1-phenyl-1-deoxy-2,3,5-tri-O-benzyl-D-arabinofuranose (173 mg, 0.36 mmol, 65%): *R*_f = 0.80 (25/75 Et₂O/petroleum ether). α -Anomer: ¹H NMR (400 MHz, CDCl₃) δ 7.45–7.37 (m, 2H, CH_{Ar} Ph), 7.37–7.15 (m, 18H, CH_{Ar} Bn, CH_{Ar} Ph), 4.98 (d, *J* = 6.1 Hz, 1H, C-1), 4.58 (s, 2H, CH₂ Bn), 4.55 (d, *J* = 11.8 Hz, 1H, CHH Bn), 4.51 (d, *J* = 11.9 Hz, 1H, CHH Bn), 4.45 (d, *J* = 11.7 Hz, 1H, CHH Bn), 4.43–4.39 (m, 2H, C-4, CHH Bn), 4.21 (t, *J* = 4.1 Hz, 1H, C-3), 4.13 (dd, *J* = 6.1, 4.0 Hz, 1H, C-2), 3.69–3.61 (m, 2H, C-5); ¹³C NMR (101 MHz, CDCl₃) δ 140.6 (C_q Ph), 138.2, 137.9, 137.8 (C_q Bn), 128.5, 128.5, 128.4, 128.2, 127.9, 127.9, 127.9, 127.8, 127.8, 127.7, 127.7, 127.6, 127.6, 127.6, 126.5 (CH_{Ar} Bn, CH_{Ar} Ph), 90.3 (C-2), 85.1 (C-3), 83.9 (C-1), 81.9 (C-4), 73.5, 72.3, 72.0 (3× CH₂ Bn), 70.3 (C-5). β -Anomer: ¹H NMR (400 MHz, CDCl₃) δ 7.46–7.37 (m, 2H, CH_{Ar} Ph), 7.36–7.15 (m, 16H, CH_{Ar} Bn, CH_{Ar} Ph), 6.91–6.85 (m, 2H, CH_{Ar} Ph), 5.10 (d, *J* = 3.7 Hz, 1H, C-1), 4.62 (d, *J* = 12.1 Hz, 1H, CHH Bn), 4.58 (d, *J* = 11.8 Hz, 1H, CHH Bn), 4.55 (d, *J* = 12.1 Hz, 1H, CHH Bn), 4.52–4.49 (m, 1H, CHH Bn), 4.27–4.22 (m, 1H, C-4), 4.07 (d, *J* = 12.2 Hz, 1H, CHH Bn), 4.04–4.02 (m, 1H, C-3), 4.00–3.94 (m, 2H, CHH Bn, C-2), 3.79 (dd, *J* = 9.9, 5.9 Hz, 1H, C-5a), 3.71–3.67 (m, 1H, C-5b); ¹³C NMR (101 MHz, CDCl₃) δ 138.4 (C_q Ph), 137.9, 137.8, 136.7 (C_q Bn), 128.5, 128.5, 128.4, 128.2, 127.9, 127.9, 127.8, 127.8, 127.7, 127.7, 127.6, 127.6, 126.5 (CH_{Ar} Bn, CH_{Ar} Ph), 85.1 (C-3), 84.2 (C-2), 83.3 (C-1), 82.5 (C-4), 73.4, 71.7, 71.6 (3× CH₂ Bn), 70.6 (C-5); IR (neat) 734, 1028, 1093, 1454, 1496, 2858; HRMS (ESI) [M + Na]⁺ calcd for C₃₂H₃₂O₄ 503.21928, found 503.21863.

2,3,5-Tri-O-benzyl-D-xylo-1,4-lactone (6). 2,3,5-Tri-O-benzyl-D-xylofuranose (6.9 g, 16.4 mmol) was dissolved in DMSO (25 mL, 345 mmol). Ac₂O (16 mL, 172 mmol) was added, and the reaction was stirred at room temperature for 44 h after which TLC analysis indicated full conversion. The reaction mixture was quenched with ice water and extracted with Et₂O, and the organic layer washed with H₂O and brine, dried over MgSO₄, filtered, and concentrated. The residue was purified by silica gel column chromatography (7.5–12.5% EtOAc/petroleum ether) to provide the title compound (6.5 g, 15.5 mmol, 95% yield) as a white solid which was recrystallized from MeOH to provide an analytical sample: *R*_f = 0.80 (25/75 EtOAc/petroleum ether); ¹H NMR (400 MHz, CDCl₃) δ 7.44–7.17 (m, 15H, CH_{Ar} Bn), 5.04 (d, *J* = 11.5 Hz, 1H, CHH Bn), 4.69 (d, *J* = 11.4 Hz, 1H, CHH Bn), 4.65 (d, *J* = 11.9 Hz, 1H, CHH Bn), 4.60–4.48 (m, 5H, C-4, C-2, 3× CHH Bn), 4.36 (t, *J* = 7.1 Hz, 1H, C-2), 3.76 (dd, *J* = 10.9, 2.8 Hz, 1H, C-5a), 3.70 (dd, *J* = 10.9, 3.2 Hz, 1H, C-5b); ¹³C NMR (101 MHz, CDCl₃) δ 173.4 (C=O), 137.7, 137.4, 137.2 (C_q Bn), 128.6, 128.6, 128.5, 128.4, 128.2, 128.2, 127.8, 127.8, 127.7 (CH_{Ar} Bn), 79.5 (C-3), 77.4 (C-2, C-4), 73.7, 72.8, 72.7 (3× CH₂ Bn), 67.2 (C-5); [α]_D²⁰ = 91.9 (*c* = 1, CHCl₃); IR (neat) 608, 625, 646, 671, 698, 743, 799, 835, 864, 912, 930, 972, 993, 1024, 1070, 1088, 1105, 1128, 1188, 1213, 1242, 1285, 1344, 1377, 1393, 1454, 1466, 1497, 1732, 1769, 2872, 2909; HRMS (ESI) [M + H⁺] calcd for C₂₆H₂₆O₅ 419.18530, found 419.18545.

1-Methyl-2,3,5-tri-O-benzyl-D-xylofuranose (12). 2,3,5-Tri-O-benzyl-D-xylo-1,4-lactone (**6**, 252 mg, 0.60 mmol), three times coevaporated with toluene, was dissolved in anhydrous THF (2.5 mL) and cooled to −78 °C. Methyl lithium (0.41 mL, 0.66 mmol, 1.6 M in Et₂O) was added slowly. After 3 h, TLC analysis indicated full conversion. The reaction was quenched by addition of saturated aq NH₄Cl (2.5 mL), and the mixture was allowed to warm to room temperature. The suspension was extracted three times with EtOAc, and the combined organic layers were washed with brine, dried over MgSO₄, filtered, and concentrated. The residue was purified by silica gel column chromatography (20–30% EtOAc/pentane) to provide the title compound (243 mg, 0.56 mmol, 93% yield) as a colorless oil which was used directly in the next step: *R*_f = 0.55 (25/75 EtOAc/pentane).

α/β -1-Methyl-1-deoxy-2,3,5-tri-O-benzyl-D-xylofuranose (30). 1-Methyl-2,3,5-tri-O-benzyl-D-xylofuranose (**12**, 242 mg, 0.56 mmol), three times coevaporated with toluene, was dissolved in anhydrous DCM (7.2 mL) and cooled to −78 °C. Triethylsilane (116

μL , 0.73 mmol) was added before dropwise addition of $\text{BF}_3 \cdot \text{OEt}_2$ (92 μL , 0.73 mmol). The reaction was stirred for 6 days at -78°C after which TLC analysis indicated near full conversion. The reaction was quenched with saturated aq NaHCO_3 (8 mL), warmed to room temperature, and the suspension extracted with EtOAc (3 \times). The combined organic layers were washed with H_2O and brine, dried over MgSO_4 , filtered, and concentrated. The residue was purified by silica gel column chromatography (8–12% EtOAc /pentane) to provide an anomeric mixture ($\alpha/\beta = 15:85$) of the title compound (203 mg, 0.49 mmol, 87% yield) as a colorless oil: $R_f = 0.80$ (20/80 EtOAc /petroleum ether). β -Anomer: ^1H NMR (400 MHz, CDCl_3) δ 7.39–7.21 (m, 15H, CH_{Ar} Bn), 4.63 (d, $J = 12.0$ Hz, 1H, CHH Bn), 4.56 (d, $J = 12.1$ Hz, 1H, CHH Bn), 4.54–4.43 (m, 4H, 4 \times CHH Bn), 4.18 (ddd, $J = 6.5$, 5.3, 4.1 Hz, 1H, C-4), 3.99–3.91 (m, 2H, C-1, C-3), 3.81–3.76 (m, 1H, C-5a), 3.73 (dd, $J = 10.0$, 6.5 Hz, 1H, C-5b), 3.65 (dd, $J = 4.1$, 1.3 Hz, 1H, C-2), 1.35 (d, $J = 6.5$ Hz, 3H, CH_3); ^{13}C NMR (101 MHz, CDCl_3) δ 138.3, 138.1, 137.9 (3 \times C_q Bn), 128.6, 128.5, 128.5, 128.4, 128.0, 127.9, 127.9, 127.9, 127.8, 127.7, 127.6 (CH_{Ar} Bn), 82.7 (C-2), 82.1 (C-3), 78.5 (C-4), 76.2 (C-1), 73.5, 72.4, 72.0 (3 \times CH_2 Bn), 68.7 (C-5), 14.6 (CH_3), $^2J_{\text{H1-C2}} = +1.6$ Hz; IR (neat) 606, 640, 673, 696, 733, 799, 849, 910, 930, 970, 993, 1026, 1069, 1088, 1190, 1206, 1312, 1344, 1393, 1454, 1497, 1771, 2862, 2913; HRMS (ESI) [$\text{M} + \text{H}^+$] calcd for $\text{C}_{27}\text{H}_{30}\text{O}_4$ 419.22169, found 419.22142.

2,3,5-Tri-O-benzyl-1-phenyl-D-xylofuranose (13). Bromobenzene (76 μL , 0.70 mmol) was dissolved in THF (1.5 mL) and cooled to -78°C . *n*-Butyl lithium (0.45 mL, 0.70 mmol, 1.6 M in hexanes) was added slowly, and the mixture was stirred for 30 min. 2,3,5-Tri-O-benzyl-D-xylo-1,4-lactone (6, 230 mg, 0.55 mmol), three times with toluene coevaporated, in anhydrous THF (1.5 mL) was added dropwise. After 2 h, TLC analysis indicated full conversion. The reaction was quenched with saturated aq NH_4Cl (3 mL), and the suspension was extracted with EtOAc . The organic layer was washed with H_2O and brine, dried over MgSO_4 , filtered, and concentrated. The residue was purified by silica gel column chromatography (10–14% EtOAc /pentane) to provide the title compound (250 mg, 0.50 mmol, 91% yield) as a colorless oil which was used directly in the next step: $R_f = 0.55$ (20/80 EtOAc /pentane).

α/β -1-Phenyl-1-deoxy-2,3,5-tri-O-benzyl-D-xylofuranose (31). 1-Phenyl-2,3,5-tri-O-benzyl-D-xylofuranose (13, 238 mg, 0.48 mmol), three times coevaporated with toluene, was dissolved in anhydrous DCM (6.9 mL) and cooled to -78°C . Triethylsilane (103 μL , 0.65 mmol) was added followed by dropwise addition of $\text{BF}_3 \cdot \text{OEt}_2$ (82 μL , 0.65 mmol). After being stirred for 3 days at this temperature, TLC analysis indicated full conversion. The reaction was quenched with saturated aq NaHCO_3 (7 mL), allowed to warm to room temperature, and the suspension extracted with EtOAc (3 \times). The combined organic layers were washed with H_2O and brine, dried over MgSO_4 , filtered, and concentrated. The residue was purified by silica gel column chromatography (6–8% EtOAc /pentane) to provide an anomeric mixture ($\alpha/\beta = 25:75$) of the title compound (183 mg, 0.38 mmol, 79% yield) as a colorless oil: $R_f = 0.76$ (20/80 EtOAc /petroleum ether). β -Anomer: ^1H NMR (400 MHz, CDCl_3) δ 7.49–7.11 (m, 20H, CH_{Ar} Ph, CH_{Ar} Bn), 4.85 (d, $J = 4.0$ Hz, 1H, C-1), 4.67–4.39 (m, 6H, 6 \times CHH Bn), 4.40–4.35 (m, 1H, C-4), 4.09–4.05 (m, 1H, C-3), 3.99 (dd, $J = 4.1$, 1.4 Hz, 1H, C-2), 3.92 (dd, $J = 10.0$, 5.3 Hz, 1H, C-5a), 3.87 (dd, $J = 9.9$, 6.2 Hz, 1H, C-5b); ^{13}C NMR (101 MHz, CDCl_3) δ 140.7 (C_q Ph), 138.3, 138.0, 137.7 (C_q Bn), 128.5, 128.5, 128.4, 128.4, 128.4, 128.3, 127.9, 127.9, 127.8, 127.7, 127.7, 127.6, 127.5, 127.5, 126.7 (CH_{Ar} Ph, CH_{Ar} Bn), 89.6 (C-2), 86.1 (C-1), 83.3 (C-3), 80.7 (C-4), 73.6, 72.0, 71.5 (3 \times CH_2 Bn), 68.4 (C-5), $^2J_{\text{H1-C2}} = -2.3$ Hz. α -Anomer: ^1H NMR (400 MHz,

CDCl_3) δ 7.44–7.13 (m, 18H, CH_{Ar} Ph, CH_{Ar} Bn), 6.93–6.86 (m, 2H, CH_{Ar} Ph), 5.21 (d, $J = 3.5$ Hz, 1H, C-1), 4.67–4.60 (m, 1H, C-4), 4.59–4.39 (m, 4H, 4 \times CHH Bn), 4.13 (dd, $J = 4.0$, 1.2 Hz, 1H, C-2), 4.10 (d, $J = 12.3$ Hz, 1H, CHH Bn), 4.04–4.00 (m, 1H, CHH Bn), 3.96–3.93 (m, 1H, C-3), 3.84–3.75 (m, 2H, C-5); ^{13}C NMR (101 MHz, CDCl_3) δ 140.7 (C_q Ph), 138.4, 138.0, 137.8 (C_q Bn), 128.5, 128.5, 128.4, 128.4, 128.3, 127.9, 127.9, 127.8, 127.6, 127.5, 127.5 (CH_{Ar} Ph, CH_{Ar} Bn), 83.2 (C-3), 82.8 (C-2), 82.5 (C-1), 73.5, 72.5, 72.1 (3 \times CH_2 Bn), 68.6 (C-5), $^2J_{\text{H1-C2}} = +2.3$ Hz; IR (neat) 604, 646, 694, 731, 887, 908, 951, 986, 1003, 1026, 1067, 1206, 1252, 1308, 1358, 1452, 1495, 2860, 2918, 3028; HRMS (ESI) [$\text{M} + \text{H}^+$] calcd for $\text{C}_{32}\text{H}_{32}\text{O}_4$ 481.23734, found 481.23748.

2,3,5-Tri-O-benzyl-4-O-triethylsilyl-D-lyxonic N,O-Dimethylhydroxylamine (15). *N,O*-dimethylhydroxylamine-HCl (506 mg, 5.2 mmol), three times coevaporated with toluene, was dissolved in anhydrous THF (8 mL) and cooled to 0°C . AlMe_3 (2 M in toluene, 2.4 mL, 4.8 mmol) was added slowly and stirred for 30 min. 2,3,5-Tri-O-benzyl-D-lyxono-1,4-lactone (7, 1.0 g, 2.40 mmol) in anhydrous THF (8 mL) was slowly added, stirred for 5 min, and allowed to warm to room temperature. After 1.5 h, TLC analysis indicated full conversion. The reaction was quenched using EtOAc , and the mixture was washed with potassium sodium tartrate (saturated aq). The aqueous layer was extracted with EtOAc , and the combined organic layers were washed with brine, dried over MgSO_4 , filtered, and concentrated. The crude 2,3,5-tri-O-benzyl-D-lyxonic *N,O*-dimethylhydroxylamide, three times coevaporated with toluene, was put under argon, dissolved in anhydrous THF (12 mL), and cooled to 0°C . Imidazole (245 mg, 3.6 mmol) was added followed by dropwise addition of triethylchlorosilane (1.0 mL, 6.0 mmol), and the mixture was stirred for 5 min at 0°C after which the mixture was allowed to warm to room temperature. After being stirred overnight, TLC analysis indicated full conversion and the reaction was quenched with saturated aq NaHCO_3 . The suspension was extracted with Et_2O , and the combined organic layers were washed with brine. The combined aqueous layers were extracted with Et_2O , and the combined organic layers were dried over MgSO_4 , filtered, and concentrated. The residue was purified by silica gel column chromatography (14–16% EtOAc /pentane) to provide the title compound (1.0 g, 1.8 mmol, 73%) as a colorless oil: $R_f = 0.60$ (20/80 EtOAc /pentane); ^1H NMR (400 MHz, CDCl_3) δ 7.38–7.17 (m, 15H, CH_{Ar} Bn), 4.88 (d, $J = 8.8$ Hz, 1H, C-2), 4.56–4.43 (m, 5H, CHH Bn), 4.40 (d, $J = 11.9$ Hz, 1H, 5 \times CHH Bn), 4.25–4.18 (m, 1H, C-4), 3.95 (dd, $J = 8.8$, 2.2 Hz, 1H, C-3), 3.61–3.46 (m, 5H, CH_3N , C-5), 3.13 (s, 3H, CH_3O), 0.92 (t, $J = 7.9$ Hz, 9H, 3 \times CH_3 TES), 0.67–0.49 (m, 6H, 3 \times CH_2 TES); ^{13}C NMR (101 MHz, CDCl_3) δ 172.3 (C=O), 138.7, 138.2, 137.7 (C_q Bn), 128.4, 128.3, 128.2, 128.2, 127.8, 127.8, 127.6, 127.5 (CH_{Ar} Bn), 80.0 (C-3), 74.9, 73.3 (2 \times CH_2 Bn), 72.7 (C-2), 71.8 (CH₂ Bn), 71.6 (C-5), 70.8 (C-4), 61.7 (NCH₃), 32.1 (OCH₃), 7.1 (CH_3 TES), 5.4 (CH_2 TES); IR (neat) 613, 694, 731, 787, 956, 999, 1076, 1090, 1142, 1238, 1454, 1663, 2874, 2951; [α]_D²⁰ -3.1 ($c = 1$, CHCl_3); HRMS (ESI) [$\text{M} + \text{H}^+$] calcd for $\text{C}_{34}\text{H}_{47}\text{NO}_6\text{Si}$ 594.32454, found 594.32451.

1-Methyl-2,3,5-tri-O-benzyl-4-O-triethylsilyl-D-lyxose (16). 2,3,5-Tri-O-benzyl-4-O-triethylsilyl-D-lyxonic *N,O*-dimethylhydroxylamide (15, 416 mg, 0.7 mmol), three times coevaporated with toluene, was dissolved in anhydrous THF (4 mL) and cooled to -78°C . Methyl lithium (0.70 mL, 1.12 mmol, 1.6 M in Et_2O) was added dropwise. After being stirred for 5 h at this temperature, TLC analysis indicated complete conversion. The reaction was quenched with saturated aq NH_4Cl , and the suspension extracted with Et_2O . The organic layer was washed with water, and the combined aqueous layers were extracted with Et_2O . The combined organic layers were washed with brine, dried over MgSO_4 , filtered, and concentrated. The residue was purified by silica gel column chromatography (4–5% EtOAc /pentane), yielding the title compound (278 mg, 0.51 mmol, 72% yield) as a colorless oil: $R_f = 0.7$ (10/90 EtOAc /pentane); ^1H NMR (400 MHz, CDCl_3) δ 7.36–7.23 (m, 15H, CH_{Ar} Bn), 4.64 (d, $J = 11.7$ Hz, 1H, CHH Bn), 4.60 (d, $J = 11.7$ Hz, 1H, CHH Bn), 4.55 (d, $J = 11.9$ Hz, 1H, CHH Bn), 4.51 (d, $J = 12.4$ Hz, 1H, CHH Bn), 4.48 (d, $J = 12.1$ Hz, 1H, CHH Bn), 4.44 (d, $J = 12.0$ Hz, 1H, CHH Bn), 4.11–4.07 (m, 1H, C-4), 4.07 (d, $J = 3.7$ Hz, 1H, C-2), 3.94 (dd, $J = 5.6$, 3.7

H_z, 1H, C-3), 3.68 (dd, *J* = 10.3, 3.7 Hz, 1H, C-5a), 3.64 (dd, *J* = 10.3, 5.6 Hz, 1H, C-5b), 2.17 (s, 3H, COCH₃), 0.89 (t, *J* = 7.9 Hz, 9H, CH₃ TES), 0.61–0.48 (m, 6H, CH₂ TES); ¹³C NMR (101 MHz, CDCl₃) δ 210.0 (C=O), 138.3, 138.3, 137.7 (C_q Bn), 128.5, 128.4, 127.9, 127.8, 127.7, 127.6 (CH_{Ar} Bn), 84.6 (C-2), 81.8 (C-3), 73.6, 73.3, 72.9 (3× CH₂ Bn), 72.6 (C-4), 72.3 (C-5), 27.9 (C=OCH₃), 7.0 (CH₃ TES), 4.9 (CH₂ TES); IR (neat) 606, 694, 731, 783, 908, 980, 1003, 1026, 1074, 1088, 1207, 1283, 1350, 1414, 1454, 1715, 2874, 2911, 2951; [α]_D²⁰ 0.8 (*c* = 1, CHCl₃); HRMS (ESI) [M + H⁺] calcd for C₃₃H₄₄O₅Si 549.30308, found 549.30337.

α-1-Methyl-1-deoxy-2,3,5-tri-O-benzyl-D-lyxofuranose (32). 1-Methyl-2,3,5-tri-O-benzyl-4-O-triethylsilyl-D-lyxose (**16**, 137 mg, 0.25 mmol), three times coevaporated with toluene, was dissolved in anhydrous DCM (3.1 mL) and cooled to –78 °C. Triethylsilane (52 μL, 0.33 mmol) was added before dropwise addition of BF₃·OEt₂ (82 μL, 0.65 mmol). After being stirred for 1 week at this temperature, TLC analysis showed partial conversion, with the remainder still being the starting material. The reaction was quenched with saturated aq NaHCO₃, allowed to warm to room temperature, and extracted with Et₂O. The organic layer was washed with water and brine, and the combined aqueous layers were extracted with Et₂O. The combined organic layers dried over MgSO₄, filtered, and concentrated. The residue was purified by silica gel column chromatography (8–13% EtOAc/pentane), yielding the title compound (46 mg, 0.11 mmol, 44% yield) as a single diastereomer: *R*_f = 0.55 (20/80 EtOAc/pentane); ¹H NMR (400 MHz, CDCl₃) δ 7.37–7.24 (m, 15H, CH_{Ar} Bn), 4.72 (d, *J* = 11.8 Hz, 1H, CHH Bn), 4.64–4.56 (m, 3H, 3× CHH Bn), 4.50 (d, *J* = 11.9 Hz, 1H, CHH Bn), 4.47 (d, *J* = 12.0 Hz, 1H, CHH Bn), 4.27–4.21 (m, 1H, C-4), 4.19–4.11 (m, 1H, C-1), 4.08 (t, *J* = 4.2 Hz, 1H, C-4), 3.74 (dd, *J* = 9.8, 5.8 Hz, 1H, C-5a), 3.67 (dd, *J* = 9.7, 6.7 Hz, 1H, C-5b), 3.55 (dd, *J* = 7.7, 4.2 Hz, 1H, C-2), 1.24 (d, *J* = 6.3 Hz, 3H, CH₃); ¹³C NMR (101 MHz, CDCl₃) δ 138.5, 138.3, 138.0 (C_q Bn), 128.5, 128.4, 128.4, 128.0, 127.9, 127.9, 127.8, 127.7, 127.7 (CH_{Ar} Bn), 85.1 (C-2), 78.6 (C-4), 77.2 (C-3), 75.6 (C-1), 73.6, 73.5, 72.7 (CH₂ Bn), 69.1 (C-5), 19.4 (CH₃), ²*J*_{H1-C2} = –3.7 Hz; [α]_D²⁰ = 26.6 (*c* = 1.1, CHCl₃); IR (neat) 696, 735, 810, 845, 914, 932, 1003, 1026, 1061, 1086, 1146, 1206, 1273, 1312, 1344, 1366, 1452, 1497, 1722, 2866, 2924, 2968; HRMS (ESI) [M + H⁺] calcd for C₂₇H₃₀O₄ 419.22169, found 419.22149.

2,3,5-Tri-O-benzyl-4-O-triethylsilyl-1-phenyl-D-lyxose (17). Bromobenzene (76 μL, 0.72 mmol) was dissolved in anhydrous THF (1 mL) and cooled to –78 °C. *n*-Butyl lithium (0.45 mL, 0.72 mmol, 1.6 M in hexanes) was added dropwise, and the mixture was stirred at this temperature for 30 min. 2,3,5-Tri-O-benzyl-4-O-triethylsilyl-D-lyxononic *N,O*-dimethylhydroxylamide (**15**, 342 mg, 0.58 mmol), three times coevaporated with toluene, in dry THF (4 mL) was added slowly, and the reaction mixture was stirred for 18 h. TLC analysis indicated full consumption of the starting material, and the reaction was quenched with saturated aq NH₄Cl. The suspension was extracted with Et₂O, and the organic layers were washed with water and brine. The combined aqueous layers were extracted with Et₂O, and the combined organic layers were dried over MgSO₄, filtered, and concentrated. The residue was purified by silica gel column chromatography (4–7% EtOAc/pentane) to provide the title compound (210 mg, 0.34 mmol, 60% yield) as a colorless oil: *R*_f = 0.80 (10/90 EtOAc/pentane); ¹H NMR (400 MHz, CDCl₃) δ 8.06–7.98 (m, 2H, *m*-CH_{Ar} Ph), 7.53–7.45 (m, 1H, *p*-CH_{Ar} Ph), 7.39–7.33 (m, 2H, *o*-CH_{Ar} Ph), 7.32–7.21 (m, 10H, CH_{Ar} Bn), 7.16–7.09 (m, 3H, CH_{Ar} Bn), 6.95–6.89 (m, 2H, CH_{Ar} Bn), 5.14 (d, *J* = 7.4 Hz, 1H, C-2), 4.56 (d, *J* = 11.2 Hz, 1H, CHH Bn), 4.45 (d, *J* = 12.0 Hz, 1H, CHH Bn), 4.42–4.34 (m, 3H, 3× CHH Bn), 4.29 (d, *J* = 11.4 Hz, 1H, CHH Bn), 4.27–4.20 (m, 1H, C-4), 4.04 (dd, *J* = 7.4, 3.1 Hz, 1H, C-3), 3.59–3.50 (m, 2H, C-5), 0.91 (t, *J* = 7.9 Hz, 9H, CH₃ TES), 0.63–0.52 (m, 6H, CH₂ TES); ¹³C NMR (101 MHz, CDCl₃) δ 200.4 (C=O), 138.1, 137.8, 137.5, 137.1 (C_q Ph, C_q Bn), 133.2 (*p*-CH_{Ar} Ph), 129.0 (*m*-CH_{Ar} Ph), 128.4, 128.3, 128.1, 128.0, 127.8, 127.8, 127.6, 127.4 (CH_{Ar} Bn, *o*-CH_{Ar} Ph), 80.9 (C-3), 79.7 (C-2), 74.2, 73.2, 72.0 (CH₂ Bn), 71.7 (C-4), 71.5 (C-5), 7.1 (CH₃ TES), 5.2 (CH₂ TES); IR (neat) 652, 694, 735, 802, 824, 845, 812, 1001, 1026, 1070, 1090, 1177, 1207, 1248, 1269, 1315, 1362, 1395, 1452, 1688, 1722, 2874,

2951; [α]_D²⁰ 3.2 (*c* = 1, CHCl₃); HRMS (ESI) [M + H⁺] calcd for C₃₈H₄₆O₅Si 611.31873, found 611.31904.

2,3,5-Tri-O-benzyl-1-deoxy-α-1-phenyl-D-lyxofuranose (33). 2,3,5-Tri-O-benzyl-4-O-triethylsilyl-1-phenyl-D-lyxose (**17**, 70 mg, 0.12 mmol), three times coevaporated with toluene, was dissolved in anhydrous DCM (1.4 mL) and cooled to –78 °C. Triethylsilane (24 μL, 0.15 mmol) was added before dropwise addition of BF₃·OEt₂ (38 μL, 0.30 mmol). After being stirred for 1 week at this temperature, TLC analysis showed partial conversion, with the remainder still being the starting material. The reaction was quenched saturated aq NaHCO₃, and the suspension was extracted with Et₂O. The organic layer was washed with water and brine, and the combined aqueous layers were extracted with Et₂O. The combined organic layers were dried over MgSO₄, filtered, and concentrated. The residue was purified by silica gel column chromatography (8–10% EtOAc/pentane), yielding the title compound (43 mg, 0.09 mmol, 77% yield) as a single diastereomer: *R*_f = 0.60 (10/90 EtOAc/pentane); ¹H NMR (400 MHz, CDCl₃) δ 7.40–7.21 (m, 18H, CH_{Ar} Bn, CH_{Ar} Ph), 7.18–7.09 (m, 2H, 2× CH_{Ar} Ph), 5.05 (d, *J* = 7.7 Hz, 1H, C-2), 4.79 (d, *J* = 11.8 Hz, 1H, CHH Bn), 4.63 (d, *J* = 11.7 Hz, 1H, CHH Bn), 4.61 (d, *J* = 11.9 Hz, 1H, CHH Bn), 4.53 (d, *J* = 11.9 Hz, 1H, CHH Bn), 4.50–4.42 (m, 2H, C-4, CHH Bn), 4.40 (d, *J* = 12.1 Hz, 1H, CHH Bn), 4.17 (t, *J* = 4.1 Hz, 1H, C-3), 3.91–3.83 (m, 2H, C-2, C-5a), 3.78 (dd, *J* = 9.8, 6.4 Hz, 1H, C-5b); ¹³C NMR (101 MHz, CDCl₃) δ 141.1 (C_q Ph), 138.4, 138.3, 137.8 (C_q Bn), 128.5, 128.5, 128.5, 128.4, 127.8, 127.7, 127.6, 126.2 (CH_{Ar} Ph, CH_{Ar} Bn), 86.2 (C-2), 81.3 (C-1), 79.6 (C-4), 77.5 (C-3), 73.7, 73.6, 72.6 (CH₂ Bn), 69.2 (C-5), ²*J*_{H1-C2} = –5.6 Hz; [α]_D²⁰ = 25.8 (*c* = 1, CHCl₃); IR (neat) 652, 694, 729, 752, 833, 887, 920, 961, 984, 1007, 1026, 1053, 1084, 1101, 1144, 1159, 1204, 1360, 1452, 1493, 2859, 2884, 2899, 2949, 3030; HRMS (ESI) [M + H⁺] calcd for C₃₂H₃₂O₄ 481.23734, found 481.23746.

■ ASSOCIATED CONTENT

📄 Supporting Information

General experimental information and ¹H, ¹³C, and 2D NMR spectra of all new compounds. This material is available free of charge via the Internet at <http://pubs.acs.org>.

■ AUTHOR INFORMATION

✉ Corresponding Authors

*E-mail: filippov@chem.leidenuniv.nl.

*E-mail: jcodee@chem.leidenuniv.nl.

✍ Author Contributions

§E.R.v.R. and P.v.D. contributed equally.

📄 Notes

The authors declare no competing financial interest.

■ ACKNOWLEDGMENTS

This work was financially supported by The Netherlands Organization for Scientific Research (NWO). Grid computing resources have been provided by BigGrid.nl, NIKHEF, and LGI. We kindly acknowledge Dr. Mark Somers for technical support.

■ REFERENCES

- (1) (a) Wu, Q. P.; Simons, C. *Synthesis* **2004**, 1533–1553. (b) Stambasky, J.; Hocek, M.; Kocovsky, P. *Chem. Rev.* **2009**, *109*, 6729–6764. (c) Wellington, K. W.; Benner, S. A. *Nucleosides, Nucleotides Nucleic Acids* **2006**, *25*, 1309–1333. (d) Charette, M.; Gray, M. W. *IUBMB Life* **2000**, *49*, 341–351. (e) Levy, D. E. Strategies towards C-Glycosides. In *The Organic Chemistry of Sugars*; Levy, D. E., Fügedi, P., Eds.; CRC Press: Boca Raton, FL, 2006; pp 269–348. (f) *C-Glycoside Synthesis*; Postema, M. H. D., Ed.; CRC Press: Boca Raton, FL, 1995. (g) Meng, W.; Ellsworth, B. A.; Nirschl, A. A.; McCann, P. J.; Patel, M.; Girotra, R. N.; Wu, G.; Sher, P. M.; Morrison, E. P.; Biller, S. A.; Zahler, R.; Deshpande, P. P.; Pullockaran,

A.; Hagan, D. L.; Morgan, N.; Taylor, J. R.; Obermeier, M. T.; Humphreys, W. G.; Khanna, A.; Discenza, L.; Robertson, J. G.; Wang, A.; Hang, S.; Wetterau, J. R.; Janovitz, E. B.; Flint, O. P.; Whaley, J. M.; Washburn, W. N. *J. Med. Chem.* **2008**, *51*, 1145–1149. (h) Roy-Burman, S.; Roy-Burman, P.; Visser, D. W. *Cancer Res.* **1968**, *28*, 1605–1610. (i) Hosoya, T.; Takashiro, E.; Matsumoto, T.; Suzuki, K. *J. Am. Chem. Soc.* **1994**, *116*, 1004–1015.

(2) (a) Cortezano-Arellano, O.; Melendez-Becerra, C. A.; Cortes, F.; Sartillo-Piscil, F.; Cordero-Vargas, A. *Carbohydr. Res.* **2014**, *393*, 51–59. (b) Calzada, E.; Clarke, C. A.; Roussinbouchard, C.; Wightman, R. H. *J. Chem. Soc., Perkin Trans. 1* **1995**, 517–518. (c) Liu, W. M.; Wise, D. S.; Townsend, L. B. *J. Org. Chem.* **2001**, *66*, 4783–4786. (d) Centrone, C. A.; Lowary, T. L. *J. Org. Chem.* **2002**, *67*, 8862–8870. (e) Sollogoub, M.; Fox, K. R.; Powers, V. E. C.; Brown, T. *Tetrahedron Lett.* **2002**, *43*, 3121–3123. (f) Terauchi, M.; Abe, H.; Matsuda, A.; Shuto, S. *Org. Lett.* **2004**, *6*, 3751–3754. (g) Peifer, M.; Berger, R.; Shurtleff, V. W.; Conrad, J. C.; MacMillan, D. W. C. *J. Am. Chem. Soc.* **2014**, *136*, 5900–5903. (h) Metobo, S. E.; Xu, J.; Saunders, O. L.; Butler, T.; Aktoudianakis, E.; Cho, A.; Kim, C. U. *Tetrahedron Lett.* **2012**, *53*, 484–486.

(3) Hernández, A. R.; Kool, E. T. *Org. Lett.* **2011**, *13*, 676–679.

(4) (a) Larsen, C. H.; Ridgway, B. H.; Shaw, J. T.; Woerpel, K. A. *J. Am. Chem. Soc.* **1999**, *121*, 12208–12209. (b) Smith, D. M.; Tran, M. B.; Woerpel, K. A. *J. Am. Chem. Soc.* **2003**, *125*, 14149–14152. (c) Smith, D. M.; Woerpel, K. A. *Org. Lett.* **2004**, *6*, 2063–2066. (d) Larsen, C. H.; Ridgway, B. H.; Shaw, J. T.; Smith, D. M.; Woerpel, K. A. *J. Am. Chem. Soc.* **2005**, *127*, 10879–10884.

(5) Jensen, H. H.; Lyngbye, L.; Jensen, A.; Bols, M. *Chem.—Eur. J.* **2002**, *8*, 1218–1226.

(6) van Rijssel, E. R.; van Delft, P.; Lodder, G.; Overkleef, H. S.; van der Marel, G. A.; Filippov, D. V.; Codée, J. D. C. *Angew. Chem., Int. Ed.* **2014**, *53*, 10381–10385.

(7) Daranas, A. H.; Napolitano, J. G.; Gavin, J. A.; Garcia, C.; Norte, M.; Fernandez, J. J. *Chem.—Eur. J.* **2011**, *17*, 6338–6347.

(8) Rhoad, J. S.; Cagg, B. A.; Carver, P. W. *J. Phys. Chem. A* **2010**, *114*, 5180–5186.

(9) Altona, C.; Sundaralingan, M. *J. Am. Chem. Soc.* **1972**, *94*, 8205–8212.

(10) Cremer, D.; Pople, J. A. *J. Am. Chem. Soc.* **1975**, *97*, 1354–1358.

(11) Frisch, M. J.; et al. *Gaussian 03*, revision E.01; Gaussian, Inc.: Wallingford, CT, 2004.

(12) The graphs of the aldofuranosyl, methyl ketofuranosyl, and phenyl ketofuranosyl oxocarbenium ions have not been normalized with respect to each other and can therefore not be compared to each other.

(13) (a) Allinger, N. L.; Hirsch, J. A.; Miller, M. A.; Tyminski, I. J. *J. Am. Chem. Soc.* **1969**, *91*, 337–343. (b) Dorigo, A. E.; Pratt, D. W.; Houk, K. N. *J. Am. Chem. Soc.* **1987**, *109*, 6591–6600.

(14) Kong, J.; et al. *Spartan '04*; Wavefunction Inc.: Irvine, CA, 2004.

(15) Kofink, C. C.; Knochel, P. *Org. Lett.* **2006**, *8*, 4121–4124.